IMMUNOLOGY

Large-scale multicenter study reveals anticitrullinated SR-A peptide antibody as a biomarker and exacerbator for rheumatoid arthritis

Yang Xie[1], Chaonan Wei[1], Dongdong Fu[2], Wei Zhang[3], Yan Du[4], Chuncui Huang[5], Shuyan Liu[1], Ranran Yao[1], Zihao He[6], Shenghua Zhang[7], Xu Jin[1,8], Bin Shen[1], Lulu Cao[1], Ping Wang[1], Xiangyu Fang[1], Xi Zheng[1], Hongying Lin[1], Xihua Wei[1], Wenhao Lin[1], Mingxin Bai[1], Danxue Zhu[1,8], Yingni Li[1], Yamin Ding[1], Huaqun Zhu[1], Hua Ye[1], Jing He[1], Yin Su[1], Yuan Jia[1], Huaxiang Wu[4], Yongfu Wang[3], Dan Xing[6], Xiaoyan Qiu[7], Zhanguo Li[1,8,9]*, Fanlei Hu[1,9,10]*

Current diagnosis and treatment of rheumatoid arthritis (RA) is still challenging. More than one-third of patients with RA could not be accurately diagnosed because of lacking biomarkers. Our recent study reported that scavenger receptor-A (SR-A) is a biomarker for RA, especially for anticyclic citrullinated peptide antibody (anti-CCP)–negative RA. Here, we further identified the B cell autoantigenic epitopes of SR-A. By a large-scale multicenter study including one training and three validation cohorts of 1954 participants, we showed that anticitrullinated SR-A peptide antibody (anti-CSP) was exclusively elevated in RA as a biomarker, particularly useful for seronegative RA. Combination of anti-CSP with anti-CCP demonstrated superior diagnostic value for RA, with sensitivity of 84.83% and specificity of 92.43%. Moreover, RA anti-CSP revealed distinct glycosylation patterns, capable of provoking inflammation in cartilage organoids and exacerbating disease progression in experimental arthritis. Together, these data identify anti-CSP as an RA autoantibody clinically applicable and actively involved in disease pathogenesis.

INTRODUCTION

Rheumatoid arthritis (RA) is a common chronic systemic autoimmune disease characterized by joint destruction, disability, and premature mortality, affecting approximately 1% of the population worldwide (*1*, *2*). Early diagnosis is crucial for preventing long-term damage and disability. Anticyclic citrullinated peptide antibody (anti-CCP) and rheumatoid factor (RF) are classical serological markers for the diagnosis of RA and have been integrated into the 2010 American College of Rheumatology/European League Against Rheumatism (ACR/EULAR) classification criteria for RA (*3*). However, their discriminating power was limited, with the sensitivity and specificity of 67 and 95% for anti-CCP and 69 and 85% for RF, respectively (*4*). Therefore, there is an unmet need to identify prospective diagnostic biomarkers for RA.

Different autoantigens have been identified for RA, including collagen, fibrinogen, vimentin, fibronectin, and α-enolase (*5*). Their posttranslational modification, in particular citrullination, is essential for the pathogenesis of RA. These citrullinated autoantigens could stimulate the secretion of autoantibodies, namely, anticitrullinated protein antibodies (ACPAs) (*6*). Anti-CCP is one of the most common ACPAs. ACPAs demonstrate arthritogenic potential and perpetuate inflammation in RA through promoting innate immune cells binding (*7*), complement system activation (*8*), neutrophil extracellular traps (NETs) formation (*9*), and osteoclasts activation (*10*). Moreover, accumulating experimental evidence revealed the contribution of the glycosylation changes of ACPAs to the systemic inflammation of RA (*11*–*13*). Several typical glycosylation patterns of ACPAs have also been identified in RA.

Scavenger receptor A (SR-A), also named macrophage scavenger receptor 1 or CD204, was initially identified as a pattern recognition receptor and mainly expressed on macrophages (*14*). Besides its role in innate immunity, accumulating evidence also indicated the functional significance of SR-A in adaptive immunity (*15*). Intriguingly, our recent study further revealed it as a promising biomarker and effector for RA (*16*). In the large-scale multicenter study, soluble SR-A demonstrated a sensitivity of 66.41% and specificity of 91.45% for the diagnosis of RA, with positive predictive value (PPV) of 80.19% and negative predictive value (NPV) of 83.94%. Furthermore, SR-A$^{-/-}$ mice were resistant to collagen-induced arthritis (CIA), with impaired T helper 17 cell response. Moreover, the elevation of SR-A could accelerate the onset of arthritis in CIA mice, whereas administration of SR-A inhibitor or blocking antibody ameliorated the severity of arthritis (*16*, *17*). These results indicate SR-A as a potential RA autoantigen. However, the autoepitopes of SR-A, especially the citrullinated forms, remain unknown, and the role of the corresponding autoantibodies also needs to be further elucidated.

In this study, we identified the citrullinated autoantigenic B cell epitopes of SR-A and further revealed the diagnostic value of the corresponding autoantibody [anticitrullinated SR-A peptide

[1]Department of Rheumatology and Immunology, Peking University People's Hospital & Beijing Key Laboratory for Rheumatism Mechanism and Immune Diagnosis (BZ0135), Beijing, China. [2]Department of Rheumatology and Immunology, Xinxiang Central Hospital, Xinxiang, China. [3]Department of Rheumatology and Immunology, First Hospital Affiliated to Baotou Medical College & Inner Mongolia Key Laboratory of Autoimmunity, Baotou, China. [4]Department of Rheumatology, the Second Affiliated Hospital, Zhejiang University School of Medicine, Hangzhou, China. [5]Key Laboratory of Epigenetic Regulation and Intervention, Institute of Biophysics, Chinese Academy of Sciences, Beijing, China. [6]Arthritis Clinical and Research Center, Peking University People's Hospital, Beijing, China. [7]Department of Immunology, School of Basic Medical Sciences, Peking University, Beijing, China. [8]Peking-Tsinghua Center for Life Sciences, Peking University, Beijing, China. [9]State Key Laboratory of Natural and Biomimetic Drugs, School of Pharmaceutical Sciences, Peking University, Beijing, China. [10]Department of Integration of Chinese and Western Medicine, School of Basic Medical Sciences, Peking University, Beijing, China.
*Corresponding author. Email: fanleihu@bjmu.edu.cn (F.H.); li99@bjmu.edu.cn (Z.L.)

antibody (anti-CSP)] through a large-scale, multicenter study. The glycosylation patterns and pathogenic effects of anti-CSP in RA were also systemically investigated.

RESULTS

The levels of anti-CSP were significantly elevated in RA

The autoantigenic B cell epitopes of SR-A were identified by BepiPred Linear Epitope Prediction 2.0 from Immune Epitope Database (IEDB) and molecular mimicry analyses, and the amino acid residues of 305 to 325 with citrullination were considered as the potential candidate (table S1). The serum level of antibody against citrullinated SR-A$_{305-325}$ peptide, named anti-CSP was first assessed in healthy individuals, patients with RA or other common rheumatic diseases, including osteoarthritis (OA), Sjögren syndrome (SS), systemic lupus erythematosus (SLE), ankylosing spondylitis (AS),

adult-onset still's disease (AOSD), psoriatic arthritis (PsA), gout, and ANCA-associated vasculitis (AAV). As indicated in Fig. 1A, compared to other patients and healthy individuals, patients with RA showed significantly higher levels of anti-CSP. Moreover, the serum level of anti-CSP was not elevated in patients with nonautoimmune inflammatory diseases (NAIDs), such as pneumonia, gastritis, pancreatitis, and cholecystitis (Fig. 1B).

The specificity of the detected anti-CSP was further validated by competitive enzyme-linked immunosorbent assay (ELISA). As shown in Fig. 1C, preincubation of RA serum with gradient concentrations of CSP significantly decreased the detected anti-CSP levels. In addition, in contrast to anti-CSP, serum antibodies to noncitrullinated SR-A peptide revealed similar levels between patients with RA and healthy individuals, further suggesting the specificity of anti-CSP and the importance of citrullination to the autoantigenicity (Fig. 1D).
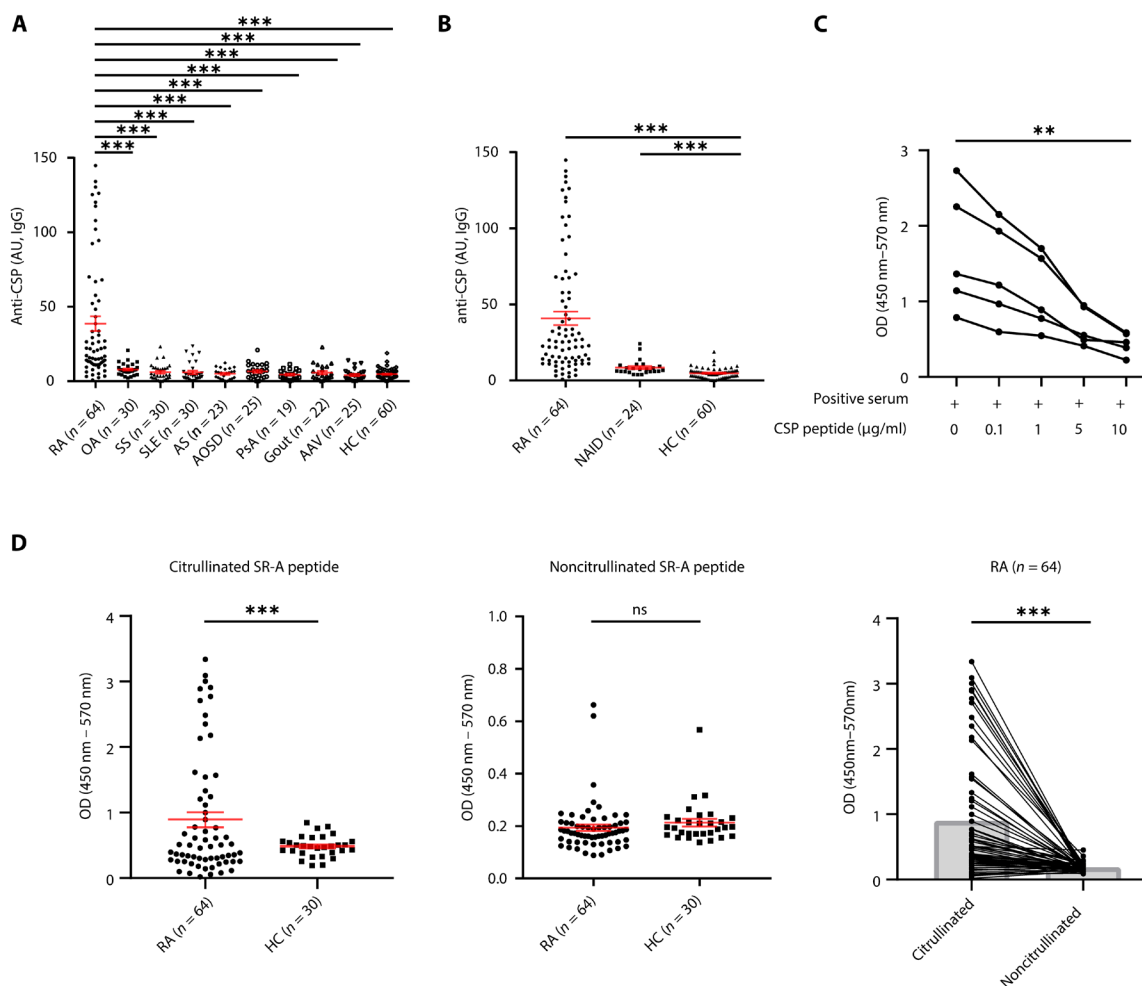

Fig. 1. The prevalence of anti-CSP in patients with RA. (A) The serum levels of anti-CSP were significantly higher in patients with RA (*n* = 64) than those in healthy controls (HCs; *n* = 60) and patients with other common rheumatic diseases and nonautoimmune inflammatory diseases (NAIDs), including osteoarthritis (OA; *n* = 30), Sjogren's syndrome (SS; *n* = 30), systemic lupus erythematosus (SLE; *n* = 30), ankylosing spondylitis (AS; *n* = 23), adult-onset still's disease (AOSD; *n* = 25), psoriatic arthritis (PsA; *n* = 19), gout (*n* = 22), and ANCA-associated vasculitis (AAV; *n* = 25). **(B)** The serum levels of anti-CSP were significantly higher in patients with RA (*n* = 64) than those in HCs (*n* = 60) and patients with NAID (*n* = 24), including enteritis, gastritis, pneumonia, and colitis. **(C)** Preincubation of RA serum (*n* = 5) with gradient concentrations of CSP peptides (0 to 10 μg/ml) significantly decreased the detected level of anti-CSP. **(D)** Comparison of the serum levels of antibody to CSP (left) and non-CSP (middle) in patients with RA (*n* = 64) and HC (*n* = 30). Red horizontal lines, means; error bars, SEMs. **P < 0.01 and ***P < 0.001; ns, not significant. Kruskal-Wallis test followed by Dunn's posttest for multiple comparisons [(A) to (C)], Mann-Whitney *U* test or Wilcoxon matched-paired signed rank test (D).

Large-scale multicenter study revealed anti-CSP as a biomarker for RA

Since anti-CSP was selectively elevated in RA, we further investigated its diagnostic value by a large-scale, multicenter study, following procedures previously described (*16*). A total of 1954 serum samples were included in the study, consisting of 832 samples in Beijing cohort (training cohort), 406 samples in Henan cohort (validation cohort 1), 400 samples in Inner Mongolia cohort (validation cohort 2), and 316 samples in Zhejiang cohort (validation cohort 3). Arbitrary unit (AU) value was used to exclude the difference of background. As shown in Fig. 2A, anti-CCP–positive patients with RA showed significantly higher levels of anti-CSP than all disease

and healthy controls (HCs) in the training cohort {median 29.44, interquartile range (IQR), 11.82 to 59.67; $P < 0.001$; odds ratio (OR), [95% confidence interval (CI) = 20.57 (13.61 to 31.09)]}. Intriguingly, anti-CCP–negative patients with RA also revealed substantially elevated levels of anti-CSP [median 17.54; IQR, 8.14 to 33.23; $P < 0.001$; OR (95% CI) = 9.61 (5.55 to 16.63); Fig. 2A]. Similar results were seen in validation cohort 1 [OR (95% CI) = 77.38 (34.03 to 175.95) for anti-CCP–positive RA and OR (95% CI) = 7.54 (2.61 to 21.73) for anti-CCP–negative RA], validation cohort 2 [OR (95% CI) = 40.69 (20.00 to 82.77) for anti-CCP–positive RA and OR (95% CI) = 22.25 (8.05 to 61.48) for anti-CCP–negative RA], and validation cohort 3 [OR (95% CI) = 24.39 (12.14 to 49.00) for
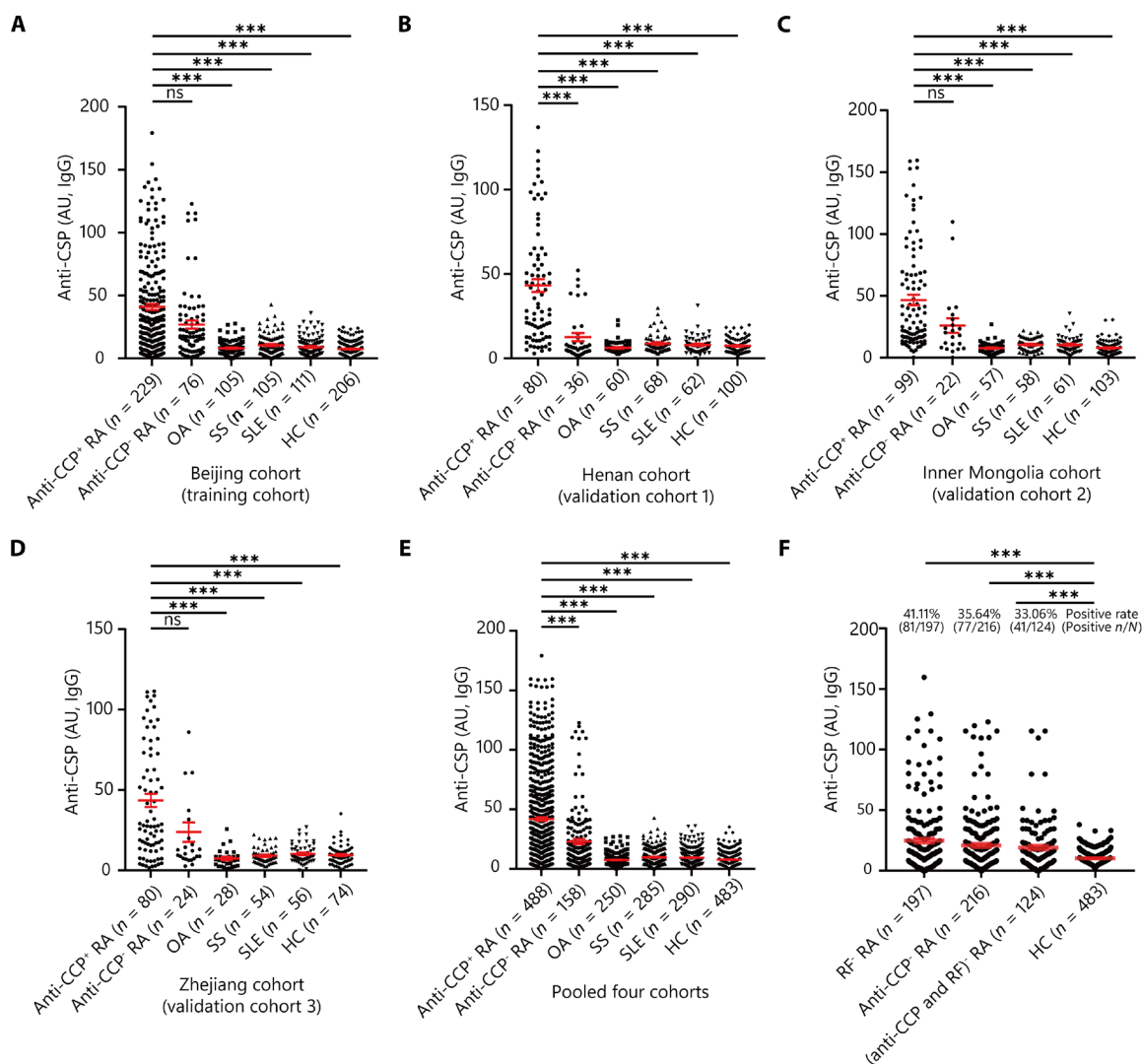

Fig. 2. The diagnostic value of anti-CSP for RA: A large-scale multicenter study. A large-scale, multicenter study was performed to access the diagnostic value of anti-CSP in RA through ELISA. The results in the training cohort, validation cohort 1, validation cohort 2, validation cohort 3, and the pooled four cohorts were shown, respectively. (**A**) Beijing cohort: training cohort (anti-CCP+ RA = 229; anti-CCP− RA = 76; OA = 105; SS = 105; SLE = 111; and HC = 206), (**B**) Henan cohort: validation cohort 1 (anti-CCP+ RA = 80; anti-CCP− RA = 36; OA = 60; SS = 68; SLE = 62; and HC = 100), (**C**) Inner Mongolia cohort: validation cohort 2 (anti-CCP+ RA = 99; anti-CCP− RA = 22; OA = 57; SS = 58; SLE = 61; and HC = 103), (**D**) Zhejiang cohort: validation cohort 3 (anti-CCP+ RA = 80; anti-CCP− RA = 24; OA = 28; SS = 54; SLE = 56; and HC = 74), (**E**) Pooled four cohorts: pooled all four cohorts' data together (anti-CCP+ RA = 488; anti-CCP− RA = 158; OA = 250; SS = 285; SLE = 290; and HC = 483). (**F**) The levels and the positive rates of patients with anti-CSP in anti-CCP–negative and/or RF-negative RA were further analyzed in a larger cohort, including patients with RF− RA (*n* = 197), patients with anti-CCP− RA (*n* = 216), and patients with (anti-CCP and RF)− RA (*n* = 124). Red horizontal lines, means; error bars, SEMs. ***$P < 0.001$; ns, not significant. Kruskal-Wallis test followed by Dunn's posttest for multiple comparisons.

anti-CCP–positive RA and OR (95% CI) = 5.41 (1.94 to 15.07) for anti-CCP–negative RA; Fig. 2, B to D]. These results were further confirmed by the pooled data from all four cohorts [OR (95% CI) = 29.90 (22.28 to 40.14) for anti-CCP–positive RA and OR (95% CI) = 9.53 (6.43 to 14.12) for anti-CCP–negative RA; Fig. 2E].

The optimal cutoff value was determined by comparing 1 SD, 2 SDs, or 3 SDs above the mean value of the HCs, as well as the Youden index and the receiver operating characteristic (ROC) curve analysis. The results showed that the cutoff value of 2 SDs above the mean value of the HCs (AU value = 18.80) revealed the best clinical applicability of sensitivity and specificity. On the basis of the cutoff value, the sensitivity and specificity for anti-CSP in anti-CCP–positive RA were 64.63% (95% bootstrap CI, 58.33 to 70.81) and 91.84% (95% bootstrap CI, 89.45 to 94.10) in Beijing cohort, 71.25% (95% bootstrap CI, 61.04 to 80.77) and 96.90% (95% bootstrap CI, 94.74 to 98.65) in Henan cohort, 64.65% (95% bootstrap CI, 55.21 to 74.14) and 95.70% (95% bootstrap CI, 93.13 to 97.86) in Inner Mongolia cohort, and 65.00% (95% bootstrap CI, 54.22 to 75.29) and 92.92% (95% bootstrap CI, 89.37 to 96.19) in Zhejiang cohort, respectively. In anti-CCP–negative RA, the sensitivity and specificity for anti-CSP were 46.05% (95% bootstrap CI, 34.62 to 57.32) and 91.84% (95% bootstrap CI, 89.48 to 94.13) in Beijing cohort, 19.44% (95% bootstrap CI, 7.14 to 33.33) and 96.90% (95% bootstrap CI, 94.81 to 98.63) in Henan cohort, 50.00% (95% bootstrap CI, 28.57 to 72.00) and 95.70% (95% bootstrap CI, 93.19 to 97.88) in Inner Mongolia cohort, and 29.17% (95% bootstrap CI, 11.54 to 50.00) and 92.92% (95% bootstrap CI, 89.35 to 96.21) in Zhejiang cohort, respectively. Analysis of the pooled four cohorts revealed the sensitivity of 65.78% (95% bootstrap CI, 61.55 to 70.06), specificity of 93.96% (95% bootstrap CI, 92.66 to 95.20), PPV of 80.25% (95% bootstrap CI, 76.29 to 84.04), and NPV of 88.04% (95% bootstrap CI, 86.27 to 89.76) for anti-CSP in patients with anti-CCP–positive RA; and the sensitivity of 37.97% (95% bootstrap CI, 30.49 to 45.51), specificity of 93.96% (95% bootstrap CI, 92.62 to 95.22), PPV of 43.17% (95% bootstrap CI, 34.75 to 51.45), and NPV of 92.61% (95% bootstrap CI, 91.19 to 93.97) for anti-CSP in anti-CCP–negative RA (Table 1). All these results suggested the remarkable diagnostic value of anti-CSP for RA.

The performance of anti-CSP was further studied in the diagnosis of anti-CCP–negative and/or RF-negative RA. Besides those anti-CCP–negative and/or RF-negative RA sera from the four training and validation cohorts, additional serum samples were further collected. A total of 197 patients with RF–negative RA, 216 patients with anti-CCP–negative RA, and 124 patients with (anti-CCP and RF)–double-negative RA were ultimately detected for anti-CSP. The results showed that the positive rate of anti-CSP was 41.11% [81 of 197, OR (95% CI) = 15.36 (9.12 to 25.87)] in RF-negative patients and 35.64% [77 of 216, OR (95% CI) = 12.19 (7.26 to 20.47)] in patients with anti-CCP–negative RA. A positive rate of 33.06% [41 of 124, OR (95% CI) = 10.87 (6.11 to 19.32)] for anti-CSP was also seen in patients with (anti-CCP and RF)–double-negative RA, suggesting it as a diagnostic biomarker distinct from RF and anti-CCP (Fig. 2F).

Anti-CSP demonstrated superior diagnostic value in combination with anti-CCP for RA

Given the diagnostic value of anti-CSP in patients with anti-CCP–negative RA, we assessed the diagnostic value of anti-CSP in combination with anti-CCP for RA following the previously shown procedures (18).

The ROC curve

ROC was first used to analyze the diagnostic capability of anti-CSP, anti-CCP, and their combination for RA, respectively. The levels of anti-CCP in each cohort were shown in Fig. 3. Analysis of the Beijing cohort yielded an area under ROC curve (AUC) of 0.813 (95% bootstrap CI, 0.778 to 0.845) for anti-CSP and an AUC of 0.909 (95% bootstrap CI, 0.884 to 0.930) for anti-CCP. The combination of anti-CSP and anti-CCP yielded an AUC of 0.931 (95% bootstrap CI, 0.910 to 0.951) (Fig. 3A). These results were further confirmed in the three validation cohorts. In Henan cohort, the AUC was 0.784 (95% bootstrap CI, 0.722 to 0.841) for anti-CSP and 0.855 (95% bootstrap CI, 0.805 to 0.902) for anti-CCP. Moreover, the combination of anti-CSP and anti-CCP revealed an AUC of 0.849 (95% bootstrap CI, 0.792 to 0.903) (Fig. 3B). In Inner Mongolia cohort, the AUC was 0.882 (95% bootstrap CI, 0.841 to 0.920) for anti-CSP, 0.947 (95% bootstrap CI, 0.912 to 0.974) for anti-CCP, and 0.965 (95% bootstrap CI, 0.937 to 0.986) for anti-CSP and anti-CCP combination, respectively (Fig. 3C). In Zhejiang cohort, the AUC was 0.789 (95% bootstrap CI, 0.726 to 0.851) for anti-CSP, 0.920 (95% bootstrap CI, 0.878 to 0.963) for anti-CCP, and 0.938 (95% bootstrap CI, 0.898 to 0.979) for anti-CSP and anti-CCP combination (Fig. 3D).

Pooling the data from the four cohorts revealed an AUC of 0.816 (95% bootstrap CI, 0.793 to 0.839) for anti-CSP and 0.913 (95% bootstrap CI, 0.897 to 0.929) for anti-CCP. Further analysis revealed that the AUC for anti-CSP and anti-CCP combination was 0.927 (95% bootstrap CI, 0.911 to 0.942) (Fig. 3E). Pairwise comparison of the ROC curves further showed that the combination of anti-CSP and anti-CCP revealed the best discriminatory ability (Fig. 3). Collectively, these results indicated that anti-CSP and anti-CCP combination revealed exceptional diagnostic accuracy, better than anti-CSP or anti-CCP alone.

Sensitivity and specificity

The sensitivity and specificity of anti-CSP and anti-CCP combination for RA diagnosis were further analyzed. As illustrated in Table 2, of the 305 patients with RA in the training cohort, 229 (75.10%) were positive for anti-CCP (95% bootstrap CI, 70.10 to 79.82), with a specificity of 97.90% (95% bootstrap CI, 96.32 to 98.88). The combination of anti-CSP and anti-CCP showed the sensitivity and specificity of 86.89% (95% bootstrap CI, 82.70 to 90.23) and 89.94% (95% bootstrap CI, 87.31 to 92.46), respectively, with improved sensitivity while remaining high specificity.

Similar results were further observed in Henan cohort. The sensitivity and specificity were 68.97% (95% bootstrap CI, 60.18 to 77.39) and 98.62% (95% bootstrap CI, 97.18 to 99.67) for anti-CCP, while 75.00% (95% bootstrap CI, 66.67 to 82.88) and 95.86% (95% bootstrap CI, 93.44 to 97.96) for anti-CSP and anti-CCP combination. The improved diagnostic accuracy for anti-CCP by measurement of anti-CSP together was also illustrated in Inner Mongolia cohort. The sensitivity and specificity were 81.00% (95% bootstrap CI, 74.79 to 88.46) and 98.57% (95% bootstrap CI, 97.05 to 99.66) for anti-CCP, while 90.90% (95% bootstrap CI, 85.47 to 95.73) and 92.96% (95% bootstrap CI, 91.79 to 97.15) for anti-CSP and anti-CCP combination, respectively. Similarly, in Zhejiang cohort, the combination of anti-CSP could increase the sensitivity of anti-CCP from 76.92% (95% bootstrap CI, 68.52 to 84.68) to 84.61% (95% bootstrap CI, 76.27 to 90.43), with a modest decrease in specificity from 98.11% (95% bootstrap CI, 96.10 to 99.55) to 91.51% (95% bootstrap CI, 87.56 to 95.07). In the pooled four cohorts, the diagnostic sensitivity of anti-CSP and anti-CCP combination was 84.83% (95% bootstrap

Table 1. Sensitivity, specificity, PPV, and NPV of anti-CSP for RA diagnosis. RA, rheumatoid arthritis; OA, osteoarthritis; SS, Sjögren's syndrome; SLE, systemic lupus erythematosus; HC, healthy control; N, the number of total patients; n, the number of anti-CSP–positive patients; PPV, positive predictive value; NPV, negative predictive value; anti-CCP, anticyclic citrullinated peptide antibody; anti-CSP, anticitrullinated SR-A peptide antibody.

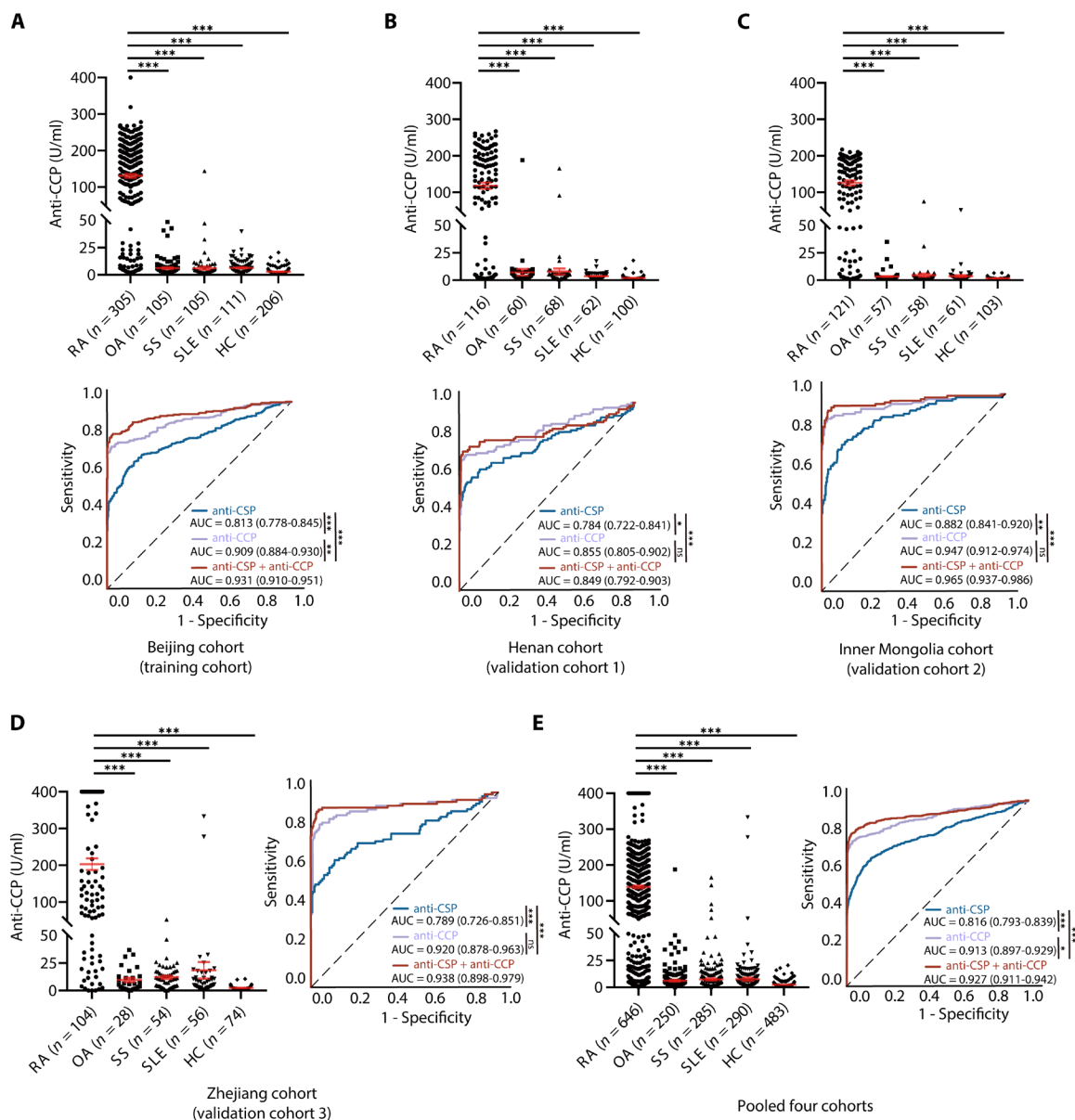| Cohorts	Groups	Total (N)	Positive (n)	Sensitivity (95% bootstrap CI), %	Specificity (95% bootstrap CI), %	PPV (95% bootstrap CI), %	NPV (95% bootstrap CI), %
Beijing cohort (training cohort)	Total RA	305	183	60.00 (54.44–65.45)	91.84 (89.43–94.11)	80.97 (75.58–86.01)	79.87 (76.53–83.07)
	CCP⁺ RA	229	148	64.63 (58.33–70.81)	91.84 (89.45–94.10)	77.49 (71.43–83.24)	85.66 (82.72–88.48)
	CCP⁻ RA	76	35	46.05 (34.62–57.32)	91.84 (89.48–94.13)	44.87 (33.82–55.88)	92.19 (89.77–94.43)
	OA	105	6	5.71			
	SS	105	13	12.38			
	SLE	111	13	11.71			
	HC	206	11	6.31			
Henan cohort (validation cohort 1)	Total RA	116	64	55.17 (45.97–64.10)	96.90 (94.74–98.65)	87.67 (79.71–94.74)	84.38 (80.42–88.13)
	CCP⁺ RA	80	57	71.25 (61.04–80.77)	96.90 (94.74–98.65)	86.36 (77.42–94.03)	92.43 (89.30–95.27)
	CCP⁻ RA	36	7	19.44 (7.14–33.33)	96.90 (94.81–98.63)	43.75 (18.75–68.42)	90.65 (87.34–93.83)
	OA	60	2	3.33			
	SS	68	5	13.16			
	SLE	62	1	1.61			
	HC	100	1	1.00			
Inner Mongolia cohort (validation cohort 2)	Total RA	121	75	62.00 (53.17–70.68)	95.70 (93.23–97.90)	86.20 (78.57–93.18)	85.30 (81.29–89.07)
	CCP⁺ RA	99	64	64.65 (55.21–74.14)	95.70 (93.13–97.86)	84.21 (75.44–92.06)	88.41 (84.69–91.96)
	CCP⁻ RA	22	11	50.00 (28.57–72.00)	95.70 (93.19–97.88)	47.83 (26.67–69.57)	96.04 (93.55–98.21)
	OA	57	1	1.75			
	SS	58	3	5.17			
	SLE	61	4	6.56			
	HC	103	4	3.88			
Zhejiang cohort (validation cohort 3)	Total RA	104	59	56.73 (46.90–66.29)	92.92 (89.22–96.19)	79.73 (70.31–88.46)	81.40 (76.35–86.19)
	CCP⁺ RA	80	52	65.00 (54.22–75.29)	92.92 (89.37–96.19)	77.61 (67.19–87.27)	87.56 (83.10–91.70)
	CCP⁻ RA	24	7	29.17 (11.54–50.00)	92.92 (89.35–96.21)	31.82 (12.50–53.33)	92.06 (88.21–95.41)
	OA	28	1	3.57			
	SS	54	5	9.26			
	SLE	56	4	7.14			
	HC	74	5	6.76			
Pooled four cohorts	Total RA	646	380	58.98 (55.18–62.75)	93.96 (92.65–95.22)	82.82 (79.34–86.14)	82.26 (80.26–84.15)
	CCP⁺ RA	488	321	65.78 (61.55–70.06)	93.96 (92.66–95.20)	80.25 (76.29–84.04)	88.04 (86.27–89.76)
	CCP⁻ RA	158	60	37.97 (30.49–45.51)	93.96 (92.62–95.22)	43.17 (34.75–51.45)	92.61 (91.19–93.97)
	OA	250	10	4.00			
	SS	285	26	9.12			
	SLE	290	22	7.59			
	HC	483	21	4.35			

Fig. 3. ROC curves of anti-CSP, anti-CCP, and their combination for RA diagnosis. Anti-CCP levels and receiver operating characteristic (ROC) curves of anti-CSP, anti-CCP, and anti-CSP and anti-CCP combination (RA versus all controls) in the training cohort (**A**), validation cohort 1 (**B**), validation cohort 2 (**C**), validation cohort 3 (**D**), and the pooled four cohorts (**E**) were shown, respectively. The 95% bootstrap confidence intervals (CIs) for the AUCs were indicated within parentheses. Red horizontal lines, means; error bars, SEMs. *$P < 0.05$, **$P < 0.01$, and ***$P < 0.001$; ns, not significant. Kruskal-Wallis test followed by Dunn's posttest for multiple comparisons and Delong method for ROC comparisons. Anti-CCP, anticyclic citrullinated peptide antibody; AUC, area under the ROC curve.

CI, 82.05 to 87.54), with a high specificity of 92.43% (95% bootstrap CI, 91.06 to 93.89), PPV of 84.69% (95% bootstrap CI, 81.99 to 87.50), and NPV of 92.50% (95% bootstrap CI, 91.03 to 93.88). Compared with other emerging biomarkers, anti-CSP revealed comparable or better diagnostic values. Its combination with anti-CCP confers superior diagnostic efficiency for RA (table S2).

Anti-CSP illustrated considerable diagnostic value in special types of RA

The diagnostic value of anti-CSP in special types of RA, including erythrocyte sedimentation rate (ESR) and/or C-reactive protein

(CRP) normal RA, early RA (ERA), and undifferentiated arthritis (UA) was further analyzed, as described previously (*16*).

Diagnostic value in ESR and/or CRP normal RA

ESR and CRP are routinely used in the diagnosis and assessment of disease activity in RA, as in the ACR/EULAR 2010 classification criteria. The performance of anti-CSP was then compared with ESR and CRP. The levels of anti-CSP and the positive rates in patients with RA with increased ESR/CRP or normal ESR/CRP from the training and validation cohorts were further analyzed. The results elucidated the elevated levels of anti-CSP with high prevalence in patients with RA with increased ESR and increased CRP [OR (95%

Table 2. Diagnostic value of anti-CSP, anti-CCP, and their combination for RA. RA, rheumatoid arthritis; anti-CSP, anticitrullinated SR-A peptide antibody; anti-CCP, anticyclic citrullinated peptide antibody; PPV, positive predictive value; NPV, negative predictive value; CI, confidence intervals.

Cohorts	Diagnostic value	Anti-CSP	Anti-CCP	Anti-CSP or anti-CCP	Anti-CSP and anti-CCP
Beijing cohort (training cohort)	Sensitivity (95% bootstrap CI), %	60.00 (54.44–65.45)	75.10 (70.10–79.82)	86.89 (82.70–90.23)	48.52 (42.86–54.28)
	Specificity (95% bootstrap CI), %	91.84 (89.43–94.11)	97.90 (96.32–98.88)	89.94 (87.31–92.46)	99.62 (99.04–100.00)
	PPV (95% bootstrap CI), %	80.97 (75.58–86.01)	95.39 (91.98–97.55)	83.33 (78.95–87.30)	98.67 (96.55–100.00)
	NPV (95% bootstrap CI), %	79.87 (76.53–83.07)	87.01 (84.35–89.76)	92.21 (89.68–94.29)	76.98 (73.85–80.17)
Henan cohort (validation cohort 1)	Sensitivity (95% bootstrap CI), %	55.17 (45.97–64.10)	68.97 (60.18–77.39)	75.00 (66.67–82.88)	49.14 (40.00–58.42)
	Specificity (95% bootstrap CI), %	96.90 (94.74–98.65)	98.62 (97.18–99.67)	95.86 (93.44–97.96)	99.66 (98.92–100.00)
	PPV (95% bootstrap CI), %	87.67 (79.71–94.74)	95.24 (90.24–98.90)	87.88 (81.25–93.94)	98.28 (94.12–100.00)
	NPV (95% bootstrap CI), %	84.38 (80.42–88.13)	88.82 (85.23–92.21)	90.55 (87.09–93.75)	83.05 (79.01–86.86)
Inner Mongolia cohort (validation cohort 2)	Sensitivity (95% bootstrap CI), %	62.00 (53.17–70.68)	81.00 (74.79–88.46)	90.90 (85.47–95.73)	52.89 (43.90–61.61)
	Specificity (95% bootstrap CI), %	95.70 (93.23–97.90)	98.57 (97.05–99.66)	92.96 (91.79–97.15)	99.64 (98.88–100.00)
	PPV (95% bootstrap CI), %	86.20 (78.57–93.18)	96.08 (91.92–99.11)	87.30 (81.82–93.50)	98.46 (94.81–100.00)
	NPV (95% bootstrap CI), %	85.30 (81.29–89.07)	92.28 (89.47–95.49)	95.99 (93.53–98.17)	82.98 (78.98–86.93)
Zhejiang cohort (validation cohort 3)	Sensitivity (95% bootstrap CI), %	56.73 (46.90–66.29)	76.92 (68.52–84.68)	84.61 (76.27–90.43)	50.00 (40.37–59.80)
	Specificity (95% bootstrap CI), %	92.92 (89.22–96.19)	98.11 (96.10–99.55)	91.51 (87.56–95.07)	99.53 (98.51–100.00)
	PPV (95% bootstrap CI), %	79.73 (70.31–88.46)	95.29 (90.12–98.89)	84.21 (75.27–89.81)	98.11 (93.65–100.00)
	NPV (95% bootstrap CI), %	81.40 (76.35–86.19)	90.04 (85.53–93.39)	96.04 (88.07–95.43)	80.23 (75.38–84.98)
Pooled cohorts	Sensitivity (95% bootstrap CI), %	58.98 (55.18–62.75)	76.01 (72.23–78.77)	84.83 (82.05–87.54)	49.69 (45.75–53.51)
	Specificity (95% bootstrap CI), %	93.96 (92.65–95.22)	98.39 (97.24–98.84)	92.43 (91.06–93.89)	99.62 (99.24–99.92)
	PPV (95% bootstrap CI), %	82.82 (79.34–86.14)	93.07 (93.42–97.03)	84.69 (81.99–87.50)	98.47 (96.94–99.69)
	NPV (95% bootstrap CI), %	82.26 (80.26–84.15)	89.80 (87.43–90.62)	92.50 (91.03–93.88)	80.04 (77.99–81.90)

CI) = 38.02 (23.19 to 62.33)], normal ESR and increased CRP [OR (95% CI) = 53.78 (22.08 to 131)], and increased ESR and normal CRP [OR (95% CI) = 35.08 (19.25 to 63.93), Fig. 4A], respectively. Even in patients with RA with normal ESR and normal CRP, the positive rate of anti-CSP still reached 47.80% [76 of 159, OR (95% CI) = 20.15 (11.78 to 34.46) (Fig. 4A)], indicating its potential as a biomarker and disease activity indicator for RA.

Diagnostic value in ERA
Early diagnosis and effective treatment are important for timely intervention, thus preventing joint damage and disability in patients with RA. Therefore, we further analyzed the diagnostic value of anti-CSP in ERA. In those patients from the four training and validation cohorts, anti-CSP revealed a positive rate of 58.86% [103 of

175, OR (95% CI) = 31.47 (18.51 to 53.52)] and 58.62% [68 of 116, OR (95% CI) = 31.17 (17.58 to 55.25)] in patients with ERA with disease duration ≤24 and ≤12 months, respectively. Anti-CSP also demonstrated a prevalence of 52.38% [33 of 63, OR (95% CI) = 24.20 (12.51 to 46.83)] in patients with ERA with disease duration ≤6 months, further revealing its substantial diagnostic value (Fig. 4B).

Predictive value in UA
The value of anti-CSP as a predictor in serum samples from 122 patients with UA was further examined. The results showed that although lower than those in patients with ERA and RA, anti-CSP levels in patients with UA were moderately higher than those in HCs (Fig. 4C). Nine of the patients with UA [7.38%, OR (95% CI) = 31.63 (19.88 to 50.33)] were anti-CSP positive, similar to the
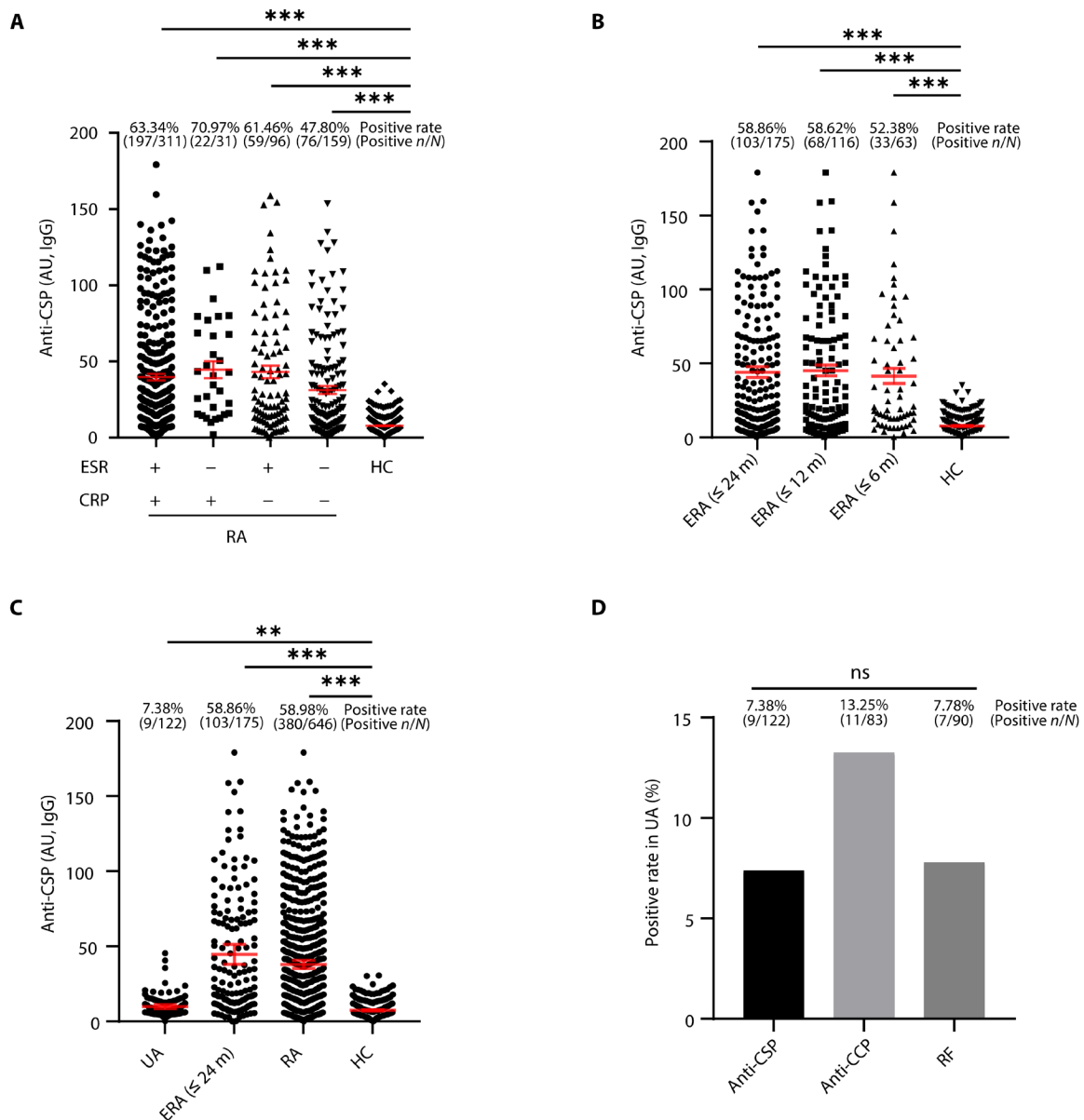
Fig. 4. Anti-CSP in RA patients with normal ESR and/or CRP, patients with ERA, and patients with UA. (**A**) The levels and the positive rates of anti-CSP in patients with RA with increased ESR (+) and increased CRP (+), normal ESR (−) and increased CRP (+), increased ESR (+) and normal CRP (−), and normal ESR (−) and normal CRP (−) were detected. (**B**) The levels and the positive rates of anti-CSP in patients with early RA (ERA), including patients with disease duration ≤24 months, disease duration ≤12 months, and disease duration ≤6 months. (**C**) The levels and the positive rates of anti-CSP in patients with undifferentiated arthritis (UA), ERA, and patients with RA were compared. (**D**) Prevalence of anti-CSP, anti-CCP, and RF in patients with UA. *n*, the number of anti-CSP–positive patients; *N*, the number of total patients. Red horizontal lines, means; error bars, SEMs. ***$P < 0.001$; ns, not significant. Kruskal-Wallis test followed by Dunn's posttest for multiple comparisons.

positive rate of anti-CCP (13.25%) and RF (7.78%), indicating the potential value of anti-CSP as a latent predictive biomarker in UA (Fig. 4D). Together, all these results suggested anti-CSP as a diagnostic biomarker for RA, facilitating an earlier and more accurate diagnosis of RA.

Anti-CSP correlated with patients with RA clinical and immunological features

The correlation of anti-CSP with clinical and immunological features of patients with RA was analyzed in both the training and

validation cohorts, as described previously (*16*). As shown in Table 3, anti-CSP was positively associated with anti-CCP, antibodies to mutated citrullinated vimentin (anti-MCV), tender joint count (TJC), swollen joint count (SJC), and disease activity score 28 (DAS28). The levels of anti-CSP were higher in patients with RA with high disease activity score (DAS28 > 5.1), elevated ESR, positive RF, and positive anti-CCP (fig. S1), further indicating the clinical value and significance of anti-CSP. In addition, according to the cutoff value (18.80), patients with RA were divided into anti-CSP–positive and anti-CSP–negative groups. Significantly higher disease activity and

Table 3. Correlation of anti-CSP with RA patient clinical and immunological features. ESR, erythrocyte sedimentation rate; CRP, C-reactive protein; anti-MCV, antimutated citrullinated vimentin; RF, rheumatoid factor; Ig, immunoglobulin; SJC, swollen joint count; TJC, tender joint count; DAS28, disease activity score 28. *$P < 0.05$, **$P < 0.01$, and ***$P < 0.001$, with exact P values shown in the table. Two-tailed Spearman's rank correlation test.

Characteristics	Training cohort		Validation cohort 1		Validation cohort 2		Validation cohort 3	
	r	P	r	P	r	P	r	P
Ages	0.017	0.760	−0.044	0.631	−0.110	0.229	0.018	0.849
Disease duration	−0.063	0.285	0.009	0.922	−0.069	0.454	0.049	0.623
ESR	0.084	0.161	0.017	0.849	−0.074	0.415	0.044	0.653
CRP	0.120	0.052	−0.064	0.500	0.106	0.244	0.079	0.425
Anti-CCP	0.201	0.0004***	0.508	<0.0001***	0.369	<0.0001***	0.328	0.0008***
Anti-MCV	0.354	0.034*	0.034	0.822	-	-	-	-
RF	−0.044	0.521	−0.023	0.808	−0.019	0.833	−0.077	0.478
IgM	−0.043	0.509	0.064	0.759	0.018	0.841	-	-
IgG	0.063	0.328	−0.167	0.435	0.036	0.693	-	-
IgA	0.154	0.018*	0.064	0.769	−0.026	0.770	-	-
TJC	0.180	0.006*	0.279	0.002**	−0.008	0.925	0.049	0.622
SJC	0.041	0.056	0.220	0.019*	−0.039	0.675	0.097	0.327
DAS28	0.169	0.010*	0.264	0.005**	0.014	0.870	0.068	0.408

anti-CCP were observed in the anti-CSP–positive group than in the anti-CSP–negative group (table S3).

The levels of anti-CSP in patients with RA before and after therapy were also detected. As shown in fig. S2, after anti–tumor necrosis factor-α (TNF-α) treatment, the levels of anti-CSP were significantly decreased. As expected, ESR and CRP also revealed remarkable decrease. However, RF and anti-CCP showed no significant changes. These results suggested the dual role of anti-CSP as RA diagnostic biomarker and disease activity indicator, showing better performance than anti-CCP, RF, ESR, and CRP.

Anti-CSP manifested a distinct *N*-glycosylation pattern in RA

To reveal the potential involvement of anti-CSP in the disease pathogenesis, anti-CSP was further purified from patients with RA for analysis. As shown in Fig. 5A, the levels of anti-CSP in RA synovial fluids were comparable to those in the sera. Therefore, the synovial fluid samples were used for anti-CSP purification. In brief, anti-CSP was subsequently purified by saturated ammonium sulfate precipitation, protein G purification, and CSP affinity chromatography column purification (Fig. 5B), the purity of which was confirmed by SDS–polyacrylamide gel electrophoresis (PAGE) and Coomassie blue staining (Fig. 5C). The activity and specificity of the purified anti-CSP were then revealed by ELISA binding analysis. The results showed that the purified anti-CSP could specifically recognize the CSP peptide in a dose-dependent manner. Intriguingly, the purified anti-CSP could also bind with the CCP peptide with lower affinity (Fig. 5D), indicating the overlap but also the unique reactivity spectrum of anti-CSP with anti-CCP. Western blot further showed that the purified anti-CSP could specifically recognize both the bovine serum albumin (BSA)–conjugated CSP peptide and the citrullinated SR-A protein (Fig. 5, E and F).

Given the fundamental role of glycosylation in modulating antibody function, the *N*-glycosylation pattern of RA patient anti-CSP,

RA patient total immunoglobulin G (IgG), and HC total IgG were then detected. Using Matrix-assisted laser desorption/ionization–time-of-flight mass spectrometry (MALDI-TOF-MS^n) analysis, 11 *N*-glycan structures were identified. On the basis of the number of galactose residues, these glycoforms could be classified into three types, namely, G0 type (no galactose residue, including A1, A2, FA2, and FA2B), G1 type (one galactose residue, including A1G1, A2G1, FA2G1, and FA2BG1), and G2 type (two galactose residues, including FA2G2, FA2BG2, and FA2G2S1). The detailed information was demonstrated in table S4. Moreover, the schematic diagram of the mass spectra for RA anti-CSP, RA IgG, and HC IgG was shown in fig. S3.

The relative intensity of each glycan was further compared among RA anti-CSP, RA IgG, and HC IgG. As shown in Fig. 5G, compared to HC IgG, eight *N*-glycans in RA anti-CSP showed substantial differences. In detail, two G0 type glycans (A1 and FA2) were notably increased, while one G0 type glycan (FA2B) was decreased. Two G1 type glycans (FA2G1 and FA2BG1) showed remarkably lower intensities, and all G2 type glycans including FA2G2, FA2BG2, and FA2G2S1 were considerably decreased. The changing tendency of the relative intensity for agalactosylated and galactosylated glycans in RA anti-CSP was consistent with that in RA IgG. Several glycoforms in anti-CSP, including FA2 and FA2G1 demonstrated more obvious change in anti-CSP than in RA IgG, which indicated the pathogenicity of anti-CSP in RA. Furthermore, the level of galactosylation among three groups was compared according to the formula: G0 / (G1 + G2 × 2) (*19*). The ratio was remarkably higher in RA anti-CSP than in HC IgG and RA IgG (Fig. 5G), demonstrating the significant galactosylation deficiency in RA anti-CSP. The present results were in accordance with previous studies on galactose residue deficiency in patients with RA, suggesting the potential involvement of anti-CSP in RA pathogenesis (*11*). Besides galactosylated glycans, more obvious changes of bisecting *N*-glycans, including FA2B, FA2BG1, and FA2BG2 were also detected
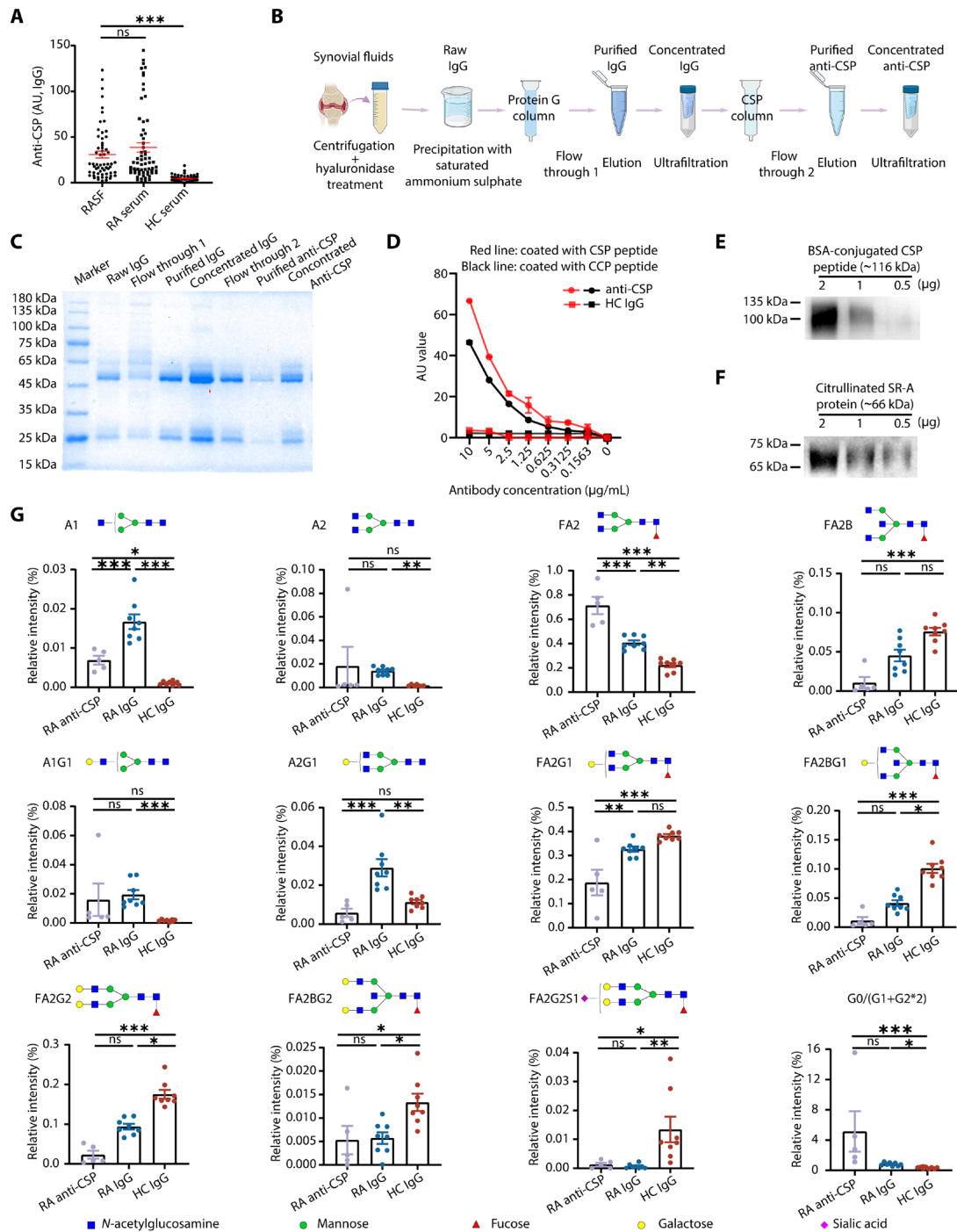
Fig. 5. Purification and *N*-glycosylation pattern analysis of RA anti-CSP. (**A**) Detection of the levels of anti-CSP in RA sera (*n* = 60) and synovial fluids (*n* = 64). (**B**) Schematic illustration of the anti-CSP purification process. Anti-CSP from synovial fluids of patients with RA was purified by centrifugation, hyaluronidase treatment, saturated ammonium sulfate precipitation, Protein G purification, CSP affinity column purification, and ultrafiltration. (**C**) SDS–polyacrylamide gel electrophoresis (SDS-PAGE) and Coomassie blue staining of different fractions during anti-CSP purification. (**D**) The specificity of anti-CSP was detected by ELISA binding analysis with CSP and CCP peptide, respectively. The results of different concentrations of anti-CSP, ranging from 0.1563 to 10 μg/ml, were shown. Red line: ELISA plate coated with CSP peptide; black line: ELISA plate coated with CCP peptide. Data are presented as mean ± SEM. The reaction of purified anti-CSP with gradient concentrations of BSA-conjugated CSP peptide (0.5 to 2 μg) (**E**) and citrullinated SR-A protein (0.5 to 2 μg) (**F**) were detected by Western blot. (**G**) Quantitative analysis of IgG glycosylation in RA anti-CSP, RA IgG and HC IgG. The results of different glycoforms, including G0 form (A1, A2, FA2, and FA2B), G1 form (A1G1, A2G1, FA2G1, and FA2BG1), and G2 form (FA2G2, FA2BG2, and FA2G2S1) were shown, respectively. The galactosylation levels were also calculated using the formula: G0/(G1 + G2 × 2). Error bars represent the SEM of each dataset. *P < 0.05, **P < 0.01, and ***P < 0.001; ns, not significant. Kruskal-Wallis test followed by Dunn's posttest for multiple comparisons [(A) and (G)] or one-way ANOVA test followed by Tukey's posttest for multiple comparisons (G).

in RA anti-CSP (Fig. 5G). These results further indicated the function of anti-CSP in the disease development, since the bisecting GlcNAc structure has been proved to be related with the ADCC effect (*20*).

Anti-CSP exacerbated the inflammation in cartilage organoids

The involvement of anti-CSP in RA pathogenesis was first assessed in cartilage organoids. The cartilage organoids were constructed using human mesenchymal stem cells (hMSCs), which were chondrogenic lineage with expression of Fc receptor and could produce certain pro-inflammatory cytokines. Cartilage organoids were generated and further stimulated with interleukin-1β (IL-1β) and TNF-α to mimic the RA inflammatory microenvironment (Fig. 6A). One month later, cartilage organoids were successfully constructed, with a diameter up to 1 mm. Hematoxylin and eosin (H&E) and Alcian blue staining of the histological sections demonstrated homogenous cell matrix distribution (Fig. 6B).

The effect of anti-CSP on cartilage organoids was further investigated. The results showed that compared to HC IgG, RA anti-CSP significantly stimulated the expression of proinflammatory cytokines, including *IL-6* and *IL-8* in the cartilage organoids as revealed by quantitative polymerase chain reaction (qPCR; Fig. 6C). These results were further confirmed by the ELISA analysis of the cartilage organoid lysates (Fig. 6D). All these results indicated the pro-inflammatory function of anti-CSP in RA. However, the involvement of anti-CSP in cartilage destruction needs to be further illustrated.

Anti-CSP promoted the development of experimental arthritis

The pathogenicity of anti-CSP was further investigated in the arthritis mice, adhering to procedures previously described (*16*). Compared to naïve mice, although lower than that in patients with RA, remarkably higher level of anti-CSP was detected in CIA mice, suggesting a cross-reaction between human and mouse (fig. S4).
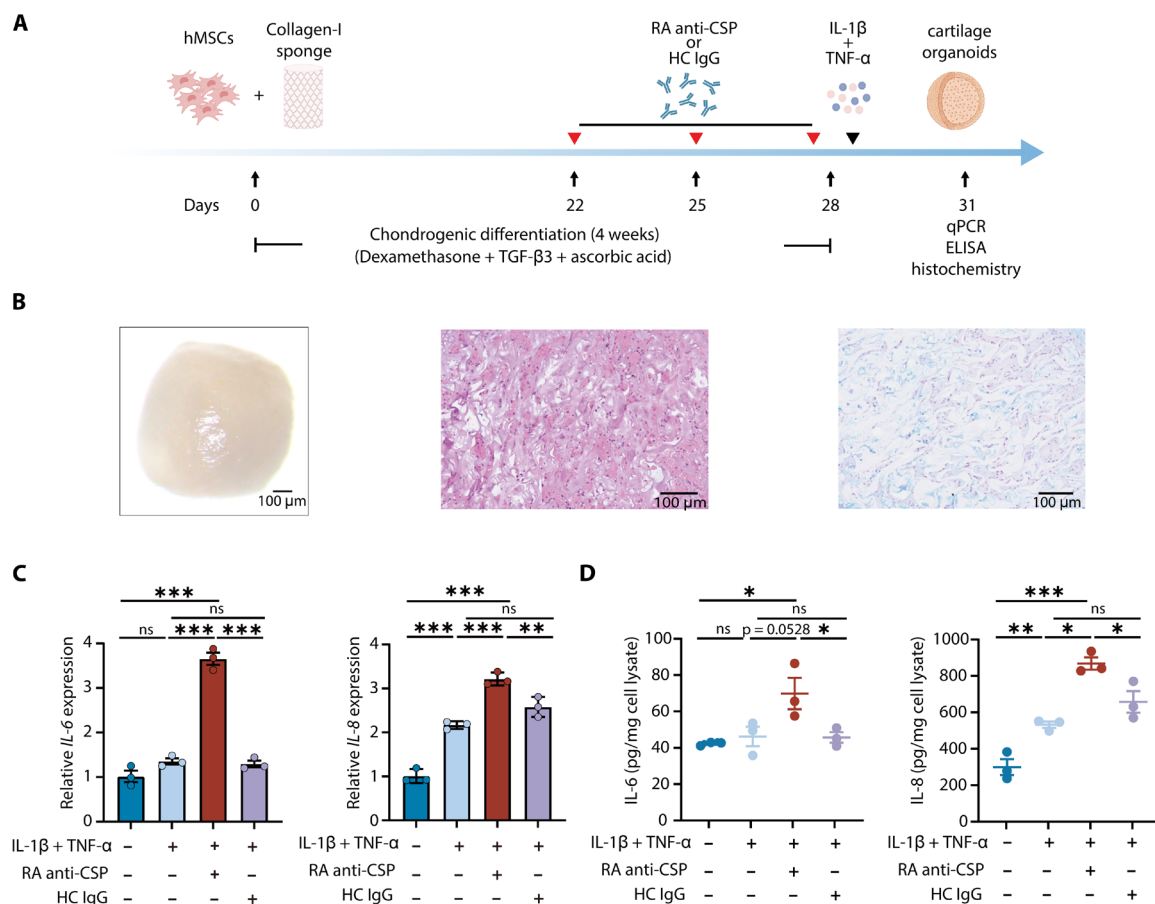

Fig. 6. RA anti-CSP exacerbated the inflammation in cartilage organoids. (**A**) Scheme of the experimental setup. hMSCs were seeded into collagen-I sponge and cultured with chrondrogenic medium containing 10 nM dexamethasone, TGF-β3 (10 ng/ml), and 10 μM ascorbic acid for 4 weeks. Purified RA anti-CSP or HC IgG (2 μg/ml) was added at day 22, 25, and 28. The cultured cartilage organoids were then stimulated with TNF-α (10 ng/ml) and IL-1β (2 ng/ml) for 3 days, and collected for qPCR, ELISA, and histochemistry analyses. (**B**) Representative images of macroscopic overview (left), H&E staining (middle), and Alcian blue staining (right) of the cartilage organoids. Scale bars, 100 μm. (**C** and **D**) Effects of RA anti-CSP on the production of IL-6 and IL-8 in cartilage organoids. Gene expression was normalized to the housekeeper gene *GAPDH*. Data are presented as means ± SEM. *$P < 0.05$, **$P < 0.01$, and ***$P < 0.001$; ns, not significant. One-way ANOVA test followed by Tukey's posttest for multiple comparisons (C and D). hMSCs, human mesenchymal stem cells; collagen-I sponge, type I collagen sponges; TGF-β3, transforming growth factor–β3; TNF-α, tumor necrosis factor–α; IL-1β, interleukin-1β.

Therefore, purified RA patient anti-CSP was then injected into CIA mice intravenously every 2 days starting from 2 days before the second immunization for a total of five injections (Fig. 7A). Subsequent analyses, as depicted in Fig. 7 (B to D), revealed that the mice receiving RA anti-CSP demonstrated significantly earlier disease onset and higher arthritis scores than those receiving HC IgG. The effect of RA anti-CSP on CIA mice was further verified by histological examination. As shown in Fig. 7E, RA anti-CSP resulted in prominent infiltration of inflammatory cells, synovial hyperplasia, and bone and cartilage destruction in the articular cavity in the CIA mice. Micro–computed tomography (CT) also demonstrated that mice receiving RA anti-CSP developed markedly more severe bone destruction in the claws and tali (Fig. 7F).

Flow cytometry analysis showed that in CIA mice receiving RA anti-CSP, the frequencies of germinal center B (GCB) cells, CD86$^+$ B cells, and CD80$^+$ B cells in the spleen, and follicular helper T (T$_{FH}$) cells in the draining lymph nodes (DLNs) were increased, indicating the activation of B cell responses (Fig. 7G). Moreover, the administration of RA anti-CSP also provoked the monocyte and neutrophil responses in CIA mice, as indicated by expanded cell frequencies in the spleen. All these results suggested the effects of anti-CSP in promoting the progression of RA.

DISCUSSION

In this study, we identified the dominant autoantigenic epitopes of SR-A, our recently identified promising diagnostic biomarker and effector of RA (16). Through a large-scale multicenter study, anti-CSP was proved to be a prospective biomarker for RA, especially useful for diagnosis of ERA and seronegative RA. Anti-CSP demonstrated distinct glycosylation patterns and could provoke inflammation in cartilage organoids and promote disease development of experimental arthritis.

Early diagnosis and intervention of RA can substantially slow the incidence of joint destruction, thus preventing irreversible disability (21, 22). Currently, several innovative biomarkers have been identified in patients with RA (table S2). Besides ACPAs, anti–modified-protein antibodies including anticarbamylated protein antibodies (anti-CarP) and anti–acetylated-protein antibodies (AAPAs) were also recognized as biomarkers and effectors of RA, with the positive rate of approximately 44.00 and 36.60%, respectively (23, 24). In addition, anti-MCV, anti-CarP, anti-AAPA, anticitrullinated α-enolase peptide 1 antibody (anti–CEP-1), and anti-peptidyl arginine deiminase 4 antibody facilitated the discrimination of 15.79, 10.40, 13.20, 20.80, and 19.00% of patients with anti-CCP–negative RA, respectively (23–27). Besides, our previous study demonstrated that soluble SR-A was an autoantigen for RA with a sensitivity of 66.41% and specificity of 91.45%, and a positivity of 49.70% in anti-CCP–negative RA (16). In this study, we further found that anti-CSP was specifically elevated in patients with RA with the sensitivity of 58.98% and the specificity of 93.96%. It showed a positive rate of 35.64% in patients with anti-CCP–negative RA and a positive rate of 33.06% in patients with anti-CCP and RF double-negative RA. The detection limit of anti-CSP is about 33 times higher than that of SR-A, therefore providing an alternative sensitive and reliable diagnostic biomarker for RA.

Moreover, the anti-CSP and anti-CCP dual combination showed substantial advantages for RA diagnosis, increasing the sensitivity of anti-CCP by 8.8% (76.01% versus 84.83%) while maintaining a high specificity of 92% (98.39% versus 92.43%). A large-scale study showed that anti-CarP and anti-CCP combination revealed a modest sensitivity of 76.00% (23). Anti–CEP-1 in combination with anti-CCP showed an increased sensitivity of 81.19%, accompanied by a lower specificity of 85.43% (26). In addition, anti-glucose-6-phosphoisomerase antibody (anti-GPI) and anti-CCP combination revealed a modest sensitivity of 85.70%, with the specificity of 64.30%, which might limit the clinical application (28). Another study demonstrated that the sensitivity of serum 14-3-3η in combination with anti-CCP were 83.00% for RA diagnosis accompanied by a lower specificity of 87.00% (29). Therefore, compared to previous studies (16, 18, 23, 25, 26, 28, 29), anti-CSP and anti-CCP combination showed superior advantages for RA diagnosis with high sensitivity and specificity (table S2). Intriguingly, although serum levels of anti-CSP and SR-A (autoantibody and autoantigen, respectively) were both elevated specifically for RA diagnosis, their levels were not parallel. Therefore, the combination of anti-CSP, SR-A, and anti-CCP may further improve the discriminating power for RA, which will be investigated in the following studies.

The diagnostic value of anti-CSP for RA offers promising perspectives for clinical application. Further investigations are still needed to translate these findings into clinical practice. The main steps include the PCT international patent applications, cooperation with GMP-certified companies for kit development, clinical trials, registration certificate application, product production, and clinical promotion. However, there still remain several obstacles to be addressed. First, the standards fulfilling the criteria to correct interassay variations should be prepared. Second, besides ELISA, the commonly used chemiluminescence method should be developed. Third, the international, large-scale multicenter validation of the diagnostic value of anti-CSP for RA in different countries, different ethnics, etc., also needs to be conducted.

Studies have shown that glycosylation profoundly influences the antibody's biology, encompassing structural stability, effector functions, and in particular immunogenicity (30). The glycosylation pattern alterations of total IgG and the disease-specific ACPA in RA have been systemically studied, and their role in the disease pathogenesis have also been investigated. The alterations of N-linked glycans both in the constant region and variable region have been reported. An array of atypical IgG glycosylation patterns has been identified in RA, characterized by reduced galactosylation, decreased sialylation, and heightened fucosylation (12). Our previous research also revealed the abnormal glycosylation forms of RA IgG and their ability to distinguish RA from OA and HC, especially for anti-CCP/RF–negative RA (31). Current theories postulate that glycosylation of antibodies may be considered as a "switch" that converts antibodies from protective to autoreactive, resulting in the progression of RA (11). The anti-inflammatory effects of galactosylation and sialylation have been well recognized. The levels of both galactosylation and sialylation of ACPA-IgG showed negative correlations with RF, CRP, and ESR level (32). Moreover, the N-linked glycans in the variable region of ACPA could predict the development of RA (33). Functional studies further showed that variable region glycosylation could change the threshold of B cells responding to self-antigens, resulting in the activation of autoimmunity and the development of RA (34). Given these findings, studies have been attempted to target the aberrant IgG glycosylation patterns for RA treatment. Conversion of endogenous IgG to anti-inflammatory mediators in vivo could significantly attenuate experimental arthritis,
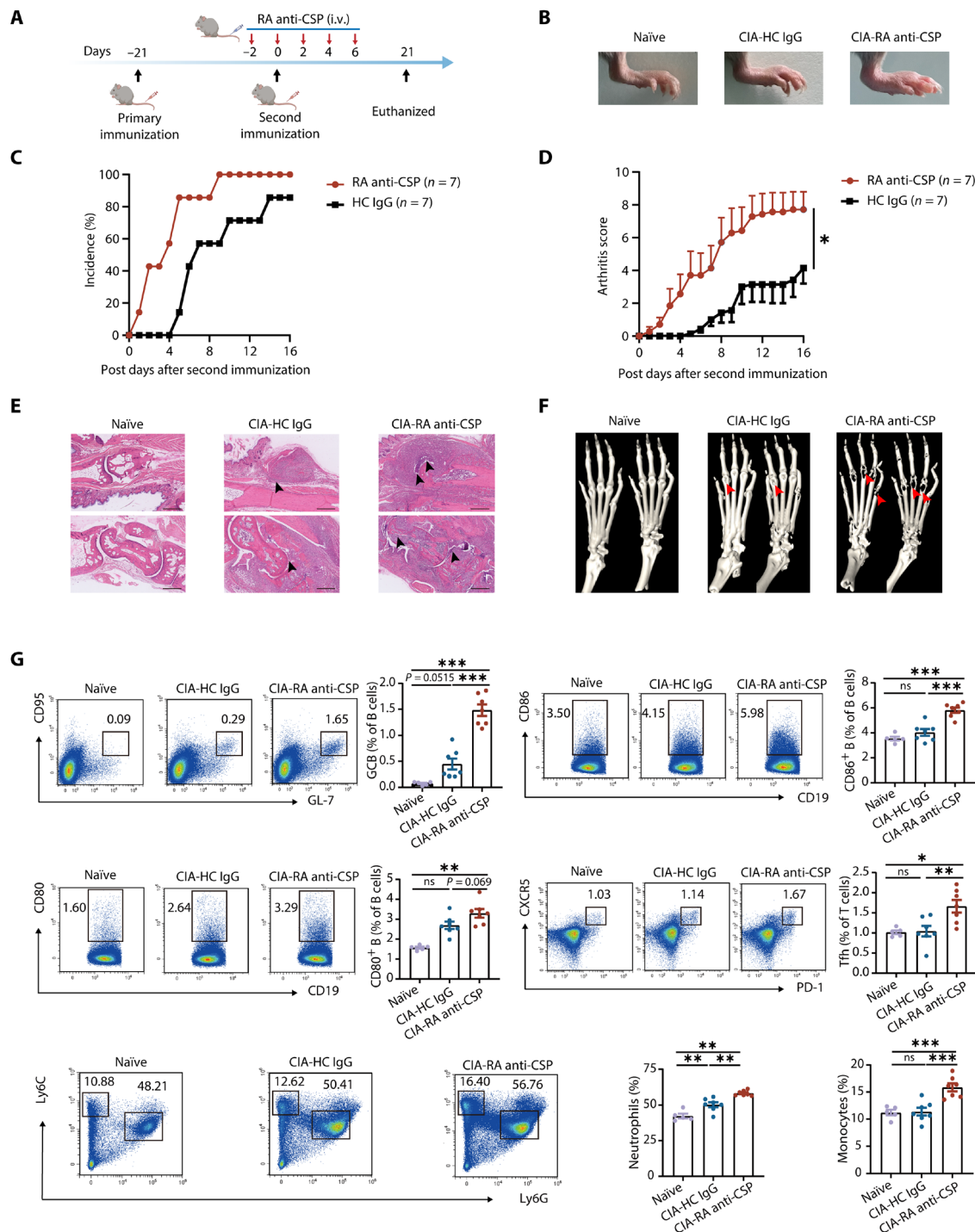
Fig. 7. RA anti-CSP promoted the development of experimental arthritis. (**A**) Scheme of the experimental setup. DBA/1 mice were intravenously injected with purified RA anti-CSP or HC IgG (2 μg per mouse) every 2 days during CIA induction, starting from 2 days before boosting immunization for a total of five times. Mice were monitored every day and euthanized 21 days after the second immunization. (**B**) Representative images of arthritic paws of naïve, CIA-RA anti-CSP, and CIA-HC IgG mice. (**C** and **D**) The arthritis incidence and the arthritis scores were shown for both CIA-RA anti-CSP and CIA-HC IgG mice over time (CIA-RA anti-CSP, $n = 7$; CIA-HC IgG, $n = 7$; $*P < 0.05$). (**E**) H&E staining of the sagittal sections of paws from naïve, CIA-RA anti-CSP, and CIA-HC IgG mice. Arrows indicate the stenosis of articular cavity and destruction of cartilage. Scale bars, 100 μm. (**F**) Micro-CT image showing the bone destruction of paws from naïve, CIA-RA anti-CSP, and CIA-HC IgG mice. (**G**) The frequencies of GCB cells, CD86$^+$ B cells, CD80$^+$ B cells, neutrophils and monocytes in the spleen, and T$_{FH}$ cells in the lymph nodes were analyzed by flow cytometry. The representative flow charts and the statistical results were shown, respectively (naïve, $n = 5$; CIA-RA anti-CSP, $n = 7$; and CIA-HC IgG, $n = 7$). Data are presented as mean ± SEM. $*P < 0.05$, $**P < 0.01$, and $***P < 0.001$; ns, not significant. Two-way repeated-measures ANOVA test (D) or one-way ANOVA test followed by Tukey's posttest for multiple comparisons (G). CIA, collagen-induced arthritis; i.v., intravenously; GCB, germinal center B cells; T$_{FH}$, follicular helper T cells.

through engineering solubilized glycosyltransferases that attach galactose or sialic acid (35). Highly sialylated collagen antibodies including ACPA demonstrated immunosuppressive properties in ameliorating joint inflammation of CIA mice. Sialidases inhibition by zanamivir was found to significantly ameliorate the severity of CIA and delay the disease onset (36). In addition, precise and rational modifications of IgG N-glycosylation by orthogonal small molecule inducers have also been attempted for allowing new recombinant protein therapeutics with tailored in vitro and in vivo effects against autoimmune diseases (37). In this study, we further detected notable disparities in the glycosylation patterns among RA anti-CSP, RA total IgG, and HC total IgG. The N-glycosylation patterns of RA anti-CSP were approximately consistent with those of RA total IgG, with more obvious changes of several glycoforms, suggesting the potential pathogenic significance of anti-CSP. Nevertheless, further functional studies are still needed to reveal the contribution of glycoforms to anti-CSP in RA pathogenesis.

The pathogenesis of anti-CSP was further analyzed through investigating the effector of RA anti-CSP on cartilage organoids. IL-1β and TNF-α as pro-inflammatory cytokines were added to mimic the inflammatory microenvironments of RA (38). RA anti-CSP showed a pro-inflammatory role in cartilage organoids, with the elevation of IL-6 and IL-8. However, in depth with more inflammatory index detected and prolonged time cultured would further confirm the role of anti-CSP. Moreover, the involvement of RA anti-CSP in cartilage destruction needs to be confirmed for further analysis, with the detection of CII or other markers. Previous study has reported anti-MCV in inducing osteoclastogenesis and bone loss in vitro and in vivo (39). Therefore, the role of RA anti-CSP in cartilage erosion would be further analyzed in other models besides cartilage organoids.

The role of anti-CSP in the development of arthritis has been revealed in mice. In CIA mice, anti-CSP could accelerate synovial hyperplasia and bone destruction concomitant with increased inflammatory cell activation. Consistent with results, Harre et al. (39) reported that human anti-MCV could induce osteoclastogenesis and bone loss in a mouse model in vivo, demonstrating the pathogenic role of ACPAs in arthritis. Some other studies also provided evidence for the arthritogenicity of ACPAs in various mouse models (40–43). However, the role of anti-CSP in other arthritis models such as collagen-antibody–induced arthritis (CAIA), serum-induced arthritis, spontaneous arthritis, etc., needs to be further investigated. Recent studies also suggested a protective role of ACPAs in arthritis. It has been reported that recombinant antibodies against citrullinated histone H2A and H4 showed anti-inflammatory activities in CAIA mice by inhibiting NETs formation and release (44). Besides, He et al. (45) identified one of the monoclonal ACPAs (clone E4), which prevented mice from CAIA by interacting with activated macrophages to promote IL-10 secretion and decrease osteoclastogenesis. In addition, anti-CSPs purified from synovial fluids of patients with RA were polyclonal antibodies. Therefore, monoclonal antibodies of anti-CSP need to be conducted to confirm the pathogenic role in RA. Moreover, the pathogenic mechanisms of anti-CSP, such as the interaction with complement and the targeted cells, should be subsequently investigated through single-cell RNA sequencing, mass cytometry analysis, and other methods. Nevertheless, the involvement and the detailed mechanisms of anti-CSP in RA pathogenesis require further investigation.

There are several limitations of our study. First, only a cross-sectional study was conducted to illustrate the diagnostic value of anti-CSP for RA. A longitudinal study should be further performed using consecutive cohorts with undiagnosed joint pain, UA, ERA, and established RA to evaluate the diagnostic value and predictive potential of anti-CSP in the future. Second, the aberrant glycosylation of anti-CSP was identified through mass spectrometry analysis. It is necessary to verify the specific change of glycosylation that is essential for the function of anti-CSP thereafter. In addition, only cartilage organoids and CIA mice were studied, and humanized mice could be further used to confirm the pathogenic effects of anti-CSP in RA.

In conclusion, our findings recognize the potential B cell autoantigenic epitopes of SR-A, our recently identified RA autoantigen, and further support the application of the antibody to citrullinated SR-A peptide (anti-CSP) for RA diagnosis, especially for patients with anti-CCP/RF–negative RA and ERA. Moreover, anti-CSP reveals pro-inflammatory role and pathogenic effects in RA, thereby providing notable insights for the diagnosis and intervention of the persistent disease.

MATERIALS AND METHODS
Study design
The B cell autoantigenic epitopes of SR-A, our recently reported RA potential biomarker and autoantigen, were identified by the bioinformative analyses. The diagnostic value of the corresponding anti-CSP was revealed by a large-scale multicenter study including one training cohort and three validation cohorts. The pathogenic effects of anti-CSP in RA were also systemically investigated by studies of cartilage organoids and arthritis mice. Sample sizes were determined by power analysis or similar studies (18, 43). All data were included in the study, with no outlier excluded. End points were prospectively selected. Unless specified, the investigators were blinded to group allocations during data collection and/or analysis, and the data were representative of three independent experiments.

Patients and samples
A total of 2307 serum samples from 739 patients with RA, 250 patients with OA, 285 patients with SS, 290 patients with SLE, 23 patients with AS, 25 patients with AOSD, 19 patients with PsA, 22 patients with gout, 25 patients with AAV, 24 patients with NAID, 122 patients with UA, and 483 HCs were collected between 2017 and 2022 at the Department of Rheumatology and Immunology, Peking University People's Hospital, Beijing, China, the Department of Rheumatology and Immunology, Xinxiang Central Hospital, Henan, China, the Department of Rheumatology and Immunology, First Hospital Affiliated to Baotou Medical College, Inner Mongolia, China, and the Department of Rheumatology, the Second Affiliated Hospital, Zhejiang University, Zhejiang, China (tables S5 to S7). All the disease and health controls were matched for age and sex with patients with RA.

While patients with RA met the 2010 ACR/EULAR classification criteria for RA, all OA (ACR, 1995), SS (ACR, 2012), SLE (SLICC Revision of ACR, 2009), AS (Modified New York criteria, 1984), gout (ACR/EULAR, 2015), PsA (CASPAR, 2006), AAV (CHCC, 2012), AOSD (Yamaguchi, 1992), UA (EULAR, 2007), and NAID patients fulfilled their classification criteria, respectively. This study was approved by the Institutional Medical Ethics Review Board of

Peking University People's Hospital, Beijing, China, the Ethical Review Board of Xinxiang Central Hospital, Henan, China, the Ethical Review Board of the First Hospital Affiliated to Baotou Medical College, Inner Mongolia, China, and the Ethical Review Board of the Second Affiliated Hospital, Zhejiang University, Zhejiang, China (2023PHB419). Informed written consents were obtained from all study participants.

SR-A B cell autoepitope identification and peptide synthesis
The protein sequence of SR-A was downloaded from National Center for Biotechnology Information (https://ncbi.nlm.nih.gov/protein/NP_619729.1). The B cell epitopes of SR-A were predicted through BepiPred Linear Epitope Prediction 2.0 from IEDB (http://tools.iedb.org/bcell/), which used a Random Forest algorithm trained on amino acids derived from crystal structure with the set threshold of 0.6 (*46*). The results revealed that amino acid residues of SR-A localized at positions 5 to 24, 301 to 341, 349 to 361, and 396 to 406 showed immunogenic capacity.

Moreover, B cell autoantigenic epitopes of RA were retrieved from the IEDB database (https://iedb.org/result_v3.php?cookie_id=45156d) and further aligned with SR-A through the protein basic local sequence alignment (BLASTp) comparative sequence analysis. With a threshold of identity ≥80%, different SR-A peptides mimicking B cell epitopes of RA were determined (table S1). In conjunction with the predicted epitopes as described above, amino acid residues of 305 to 325 of SR-A were considered to be the potential B cell autoantigenic epitope. Since citrullination is particularly important for the autoantigenicity of peptides in RA, citrullinated SR-A$_{305-325}$ (KGD-Cit-GAIGFPGS-Cit-GLPGYAG-Cit) was chosen as the potential autoantigen epitope candidate. BSA-conjugated peptides were then synthesized using the solid-phase peptide synthesis method by the Chinese Peptide Company (Hangzhou, China) for further study.

ELISA analysis of anti-CSP and anti-CCP
The concentrations of anti-CSP in serum or synovial fluid samples were measured by an ELISA assay. In brief, ELISA microplates were irradiated by ultraviolet rays overnight and then coated with CSP (10 μg/ml) at 4°C overnight. After washing, the plates were blocked with 3% BSA–phosphate-buffered saline with Tween 20 (PBST) for 2 hours at room temperature. Sera or synovial fluids were diluted 1:100 in PBST with 1% BSA and then added to the ELISA plates for 1 hour. The plates were washed again and further incubated with 100 μl of 1:13000 diluted horseradish peroxidase (HRP)–conjugated goat anti-human IgG (Zhongshan Golden Bridge Biotechnology, Beijing, China) for 30 min at 37°C. Following that, tetramethyl benzidine (Neobioscience, Beijing, China) was added and then stopped with 2 mM H$_2$SO$_4$. The optical density at 450 nm (OD$_{450}$) and OD$_{570}$ were measured with Synergy 4 Multi-Mode Microplate Reader. A mixed positive serum sample from patients with RA ($n = 15$) was included on each plate as a positive control and reference to correct interassay variations. The titer of anti-CSP was expressed as AU and quantified as follows: AU = (OD$_{anti-CSP}$ − OD$_{nonspecific\ background}$) test serum / (OD$_{anti-CSP}$ − OD$_{nonspecific\ background}$) positive control serum × 100. To keep the normalization process consistent across different study cohorts, the same positive serum was used. Moreover, the detection system of anti-CSP was validated by at least two repetitions.

To test the specificity of the ELISA analysis, sera of patients with RA with AU value of anti-CSP > 100 were selected and diluted.

Afterward, the diluted sera were preincubated with different concentrations of CSP (0 to 10 μg/ml) overnight at 4°C, and then set to anti-CSP detection as described above. In addition, antibody against noncitrullinated SR-A$_{305-325}$ peptide was also tested.

The anti-CCP was detected by the QUANTA Lite CCP3 IgG ELISA kit (REF: 704535) (Inova Diagnostics Inc., San Diego, CA, USA) that was routinely used for RA diagnosis in our four study centers, with a threshold value of 20 U/ml according to the manufacturer's recommendation.

Purification of anti-CSP
Synovial fluids from active patients with RA were centrifuged at 3500 rpm for 10 min, followed by treatment with hyaluronidase (Beijing Solarbio Science & Technology Co. Ltd., Beijing, China) for 45 min at 4°C to decrease viscosity. Then, the supernatants were precipitated by saturated ammonium sulfate with the subsequent concentration of 20, 50, and 33%. The precipitated raw IgG was dissolved and further dialyzed against PBS.

Total IgG was further purified via Protein G agarose affinity chromatography (GE Healthcare, Freiburg, Germany) and dialyzed against PBS through ultrafiltration on a Vivaspin 30 K unit (Millipore, Merck KGaA, Germany). Anti-CSP was further purified using a CSP affinity chromatography column and eluted with 0.1 M glycine-HCl buffer (pH = 2.4), followed by neutralization with 1 M Tris-HCl (pH = 9.0). The high-salt buffer of anti-CSP was exchanged against PBS through ultrafiltration on a Vivaspin 30 K unit (Millipore).

The concentration of purified anti-CSP was measured using a bicinchoninic acid assay, according to the manufacturer's instructions. The endotoxin level was detected by ToxinSensor Chromogenic LAL Endotoxin Assay Kit (Genscript, Nanjing, China), and was proved to be <1 EU/μg. Moreover, the purity of anti-CSP was verified by SDS-PAGE electrophoresis with Coomassie blue staining, while the specificity was validated by ELISA and Western blot analyses. Besides, IgG from healthy individuals and patients with RA were also purified as controls by Protein G agarose affinity chromatography (GE Healthcare) according to the manufacturer's instruction.

Glycosylation pattern analysis of anti-CSP
The identification of glycoforms of purified anti-CSP was performed as described previously (*31*). In brief, the structures of *N*-glycans of purified RA anti-CSP, RA total IgG, and healthy individual total IgG were analyzed through MALDI-TOF-MS^n GIPS strategy (*47–49*). The data of MALDI MS were obtained and normalized through MarkerView 1.2.1.1. The relative quantification was further collected and calculated by the total intensity.

Construction and treatment of cartilage organoids
The construction of cartilage organoids was performed according to the protocol as described by Martin's group (*50*). In brief, hMSCs were expanded for two passages and seeded into type I collagen sponges (Beijing Bonanga Medical Co. Ltd., Beijing, China) at a density of 5 × 10^5 cells in 15 μl in v-bottom, nonadherent 96-well plates. Cells were first cultured for 1 hour at 37°C to facilitate the distribution and adherence within the scaffolds, then cultured with chondrogenic medium containing 10 nM dexamethasone (Sigma-Aldrich, St. Louis, MO), transforming growth factor–β3 (10 ng/ml; TGF-β3, Beijing Solarbio Science & Technology Co. Ltd.) and 10 μM

ascorbic acid (Sigma-Aldrich) for 4 weeks. The medium was replaced twice per week.

On day 28, the organoids were stimulated with recombinant human TNF-α (10 ng/ml; PeproTech, Rocky Hill, NJ) and recombinant human IL-1β (2 ng/ml; PeproTech) for 3 days to mimic joint inflammation of arthritis. Purified RA anti-CSP or HC IgG was added at 2 μg/ml every 3 days, starting from 1 week before adding TNF-α and IL-1β. On day 31, the organoids were harvested for qPCR, ELISA, and histochemistry.

RNA extraction and RT-qPCR
Total RNA was extracted from the organoids using a grinding mill and TRIzol reagent, treated with deoxyribonuclease, and then examined by detecting A260/A280. After that, the RNA was reverse transcribed into cDNA, and the resulting cDNA was diluted to 10 ng/μl for qPCR (primers as in table S8). Gene expression was quantified relatively to the expression of the housekeeping gene *GAPDH*, and normalized to control by standard $2^{-\Delta\Delta CT}$ calculation (*51*).

Western blotting
Gradient concentrations of CSPs and SR-A protein (0.5, 1, and 2 μg) were separated on NuPAGE bis-tris 10% gels (Bio-Rad Laboratories) and transferred to polyvinylidene fluoride membranes. Membranes were blocked with 5% BSA-TBST and then incubated with purified anti-CSP (3 μg/ml) as primary antibody overnight at 4°C. After washing with TBST, the membranes were further incubated with HRP-conjugated goat anti-human IgG (Zhongshan Golden Bridge Biotechnology, Beijing, China) for 1 hour at room temperature. After a final wash, the membrane was developed with enhanced chemiluminescence.

ELISA assay of IL-6 and IL-8
Commercially available ELISA kits from Neobioscience Technology Co. Ltd. (Beijing, China) were used for measuring IL-6 and IL-8 in the cell lysate of cartilage organoids according to the manufacturer's instructions. The results were measured on a Synergy 4 Multi-Mode Microplate Reader with software GEN5CH 2.0 (BioTek, Winooski, VT).

Experimental arthritis induction and treatment
Six- to eight-week-old male DBA/1 mice were purchased from Huafukang Bioscience Company (Beijing, China) and housed in a specific pathogen–free environment under controlled conditions (22°C ambient temperature and 40% humidity). All animal procedures complied with relevant ethical regulations for animal research and were approved by the Institutional Animal Care and Use Committee of Peking University People's Hospital (2023PHE122).

CIA models were established in DBA/1 mice by immunization on day 1 with 200 μg of bovine type II collagen (Chondrex Inc., Redmond, WA) emulsified in complete Freund adjuvant, and on day 21 with 100 μg of bovine type II collagen emulsified in incomplete Freund adjuvant as a booster (*16*). The severity of arthritis was scored on the basis of the level of inflammation as described previously (*52*): 0, normal; 1, erythema and swelling of one or several digits; 2, erythema and moderate swelling extending from the ankle to the mid-foot (tarsals); 3, erythema and severe swelling extending from the ankle to the metatarsal joints; and 4, complete erythema and swelling encompassing the ankle, foot, and digits, resulting in deformity and/or ankyloses. The scores of all four limbs were summed, yielding a total score of 0 to 16 per mouse.

The mice received administration of purified RA patient anti-CSP or HC IgG (2 μg per mouse) intravenously every other day for a total of five times, starting from 2 days before boosting immunization. The arthritis score was recorded every day and all mice were euthanized on day 21 after the second immunization.

Flow cytometry
Mouse spleens and DLN were harvested freshly and processed to obtain single-cell suspensions. Following, the cells were set for different immune cell subset detection, including GCB cells (CD19$^+$GL-7$^+$CD95$^+$), CD80$^+$ B cells (CD19$^+$CD80$^+$), CD86$^+$ B cells (CD19$^+$CD86$^+$), monocytes (CD11b$^+$Ly6C^{hi}Ly6G$^-$), neutrophils (CD11b$^+$Ly6C^{int}Ly6G^{hi}), and T$_{FH}$ cells (CD4$^+$CXCR5$^+$PD-1^{hi}). All antibodies were purchased from BioLegend (San Diego, CA) including antimouse CD19 (catalog no. 115534), antimouse GL-7 (catalog no. 101226), antimouse CD80 (catalog no. 104706), antimouse CD86 (catalog no. 105008), antimouse CD4 (catalog no. 100414), antimouse CD86 (catalog no. 105008), antimouse CXCR5 (catalog no.145510), and antimouse PD-1 (catalog no.135210), or from eBioscience (San Diego, CA) including antimouse CD95 (catalog no. 53095182), antimouse CD11b (catalog no. 11011285), antimouse Ly6C (catalog no. 12593282), and antimouse Ly6G (catalog no. 17593182). The detailed gating strategies were shown in fig. S5. Cells were acquired and analyzed using the CytoFLEX S flow cytometer (Beckman Coulter, Brea, CA) and CytExpert software.

Mouse paw histopathology and micro-CT
Mice were euthanized and the hind paws were fixed in 4% buffered formaldehyde, decalcified in 5% EDTA, paraffin-embedded, sectioned, stained with H&E, and analyzed with NDP.view2 (Hamamatsu Photonics K.K., Japan). Micro-CT images of the mouse paws were acquired on the Tri-Modality FLEX Triumph Pre-Clinical Imaging System (Gamma Medica-Ideas, Northridge, CA). CT image set acquisitions lasted 10 min and used beam parameters of 130 μA and 80 kVp. Analyze 10.0 (AnalyzeDirect, Overland Park, KS) was used to perform the image analysis according to a previously published protocol (*16*).

Statistics
Statistical calculations were performed using the statistical software programs SPSS 26.0 (SPSS Inc., Chicago, IL) and GraphPad Prism 9 (GraphPad Software Inc., San Diego, CA). Differences between various groups were evaluated by the Mann-Whitney U test, unpaired t test, mixed-effects models, Kruskal-Wallis test followed by Dunn's posttest for multiple comparisons, one-way analysis of variance (ANOVA) test followed by Tukey's posttest, two-tailed Spearman's rank correlation test, and two-way repeated-measures ANOVA test. The effect size was calculated on the basis of OR. A pairwise comparison of ROC was performed using Delong method. The 95% confidence intervals around diagnostic value metrics were reported by bootstrap resampling, including AUC, sensitivity, specificity, PPV, and NPV. A two-sided P value of < 0.05 was considered statistically significant: $*P < 0.05$, $**P < 0.01$, and $***P < 0.001$; ns, not significant.

Supplementary Materials
The PDF file includes:
Figs. S1 to S5
Tables S1 to S8
Legend for data file S1

Other Supplementary Material for this manuscript includes the following:
Data file S1

REFERENCES AND NOTES

1. J. S. Smolen, D. Aletaha, I. B. McInnes, Rheumatoid arthritis. *Lancet* **388**, 2023–2038 (2016).

2. H. Ahsan, Origins and history of autoimmunity—A brief review. *Rheumatol. Autoimmun.* **3**, 9–14 (2023).

3. L. Van Hoovels, J. Jacobs, B. Vander Cruyssen, S. Van den Bremt, P. Verschueren, X. Bossuyt, Performance characteristics of rheumatoid factor and anti-cyclic citrullinated peptide antibody assays may impact ACR/EULAR classification of rheumatoid arthritis. *Ann. Rheum. Dis.* **77**, 667–677 (2018).

4. K. Nishimura, D. Sugiyama, Y. Kogata, G. Tsuji, T. Nakazawa, S. Kawano, K. Saigo, A. Morinobu, M. Koshiba, K. M. Kuntz, I. Kamae, S. Kumagai, Meta-analysis: Diagnostic accuracy of anti-cyclic citrullinated peptide antibody and rheumatoid factor for rheumatoid arthritis. *Ann. Intern. Med.* **146**, 797–808 (2007).

5. A. M. Curran, P. Naik, J. T. Giles, E. Darrah, PAD enzymes in rheumatoid arthritis: Pathogenic effectors and autoimmune targets. *Nat. Rev. Rheumatol.* **16**, 301–315 (2020).

6. H. U. Scherer, D. van der Woude, R. E. M. Toes, From risk to chronicity: Evolution of autoreactive B cell and antibody responses in rheumatoid arthritis. *Nat. Rev. Rheumatol.* **18**, 371–383 (2022).

7. J. Sokolove, X. Zhao, P. E. Chandra, W. H. Robinson, Immune complexes containing citrullinated fibrinogen costimulate macrophages via Toll-like receptor 4 and Fcγ receptor. *Arthritis Rheumatol.* **63**, 53–62 (2011).

8. L. A. Trouw, E. M. Haisma, E. W. Levarht, D. van der Woude, A. Ioan-Facsinay, M. R. Daha, T. W. Huizinga, R. E. Toes, Anti-cyclic citrullinated peptide antibodies from rheumatoid arthritis patients activate complement via both the classical and alternative pathways. *Arthritis Rheumatol.* **60**, 1923–1931 (2009).

9. R. Khandpur, C. Carmona-Rivera, A. Vivekanandan-Giri, A. Gizinski, S. Yalavarthi, J. S. Knight, S. Friday, S. Li, R. M. Patel, V. Subramanian, P. Thompson, P. Chen, D. A. Fox, S. Pennathur, M. J. Kaplan, NETs are a source of citrullinated autoantigens and stimulate inflammatory responses in rheumatoid arthritis. *Sci. Transl. Med.* **5**, 178ra40 (2013).

10. A. Kleyer, S. Finzel, J. Rech, B. Manger, M. Krieter, F. Faustini, E. Araujo, A. J. Hueber, U. Harre, K. Engelke, G. Schett, Bone loss before the clinical onset of rheumatoid arthritis in subjects with anticitrullinated protein antibodies. *Ann. Rheum. Dis.* **73**, 854–860 (2014).

11. Y. Rombouts, E. Ewing, L. A. van de Stadt, M. H. Selman, L. A. Trouw, A. M. Deelder, T. W. J. Huizinga, M. Wuhrer, D. van Schaardenburg, R. E. M. Toes, H. U. Scherer, Anti-citrullinated protein antibodies acquire a pro-inflammatory Fc glycosylation phenotype prior to the onset of rheumatoid arthritis. *Ann. Rheum. Dis.* **74**, 234–241 (2015).

12. H. U. Scherer, D. van der Woude, A. Ioan-Facsinay, H. el Bannoudi, L. A. Trouw, J. Wang, T. Häupl, G.-R. Burmester, A. M. Deelder, T. W. J. Huizinga, M. Wuhrer, R. E. M. Toes, Glycan profiling of anti-citrullinated protein antibodies isolated from human serum and synovial fluid. *Arthritis Rheumatol.* **62**, 1620–1629 (2010).

13. T. Kissel, R. E. M. Toes, T. W. J. Huizinga, M. Wuhrer, Glycobiology of rheumatic diseases. *Nat. Rev. Rheumatol.* **19**, 28–43 (2023).

14. M. S. Brown, J. L. Goldstein, M. Krieger, Y. K. Ho, R. G. Anderson, Reversible accumulation of cholesteryl esters in macrophages incubated with acetylated lipoproteins. *J. Cell Biol.* **82**, 597–613 (1979).

15. Y. Xie, Y. Jia, Z. Li, F. Hu, Scavenger receptor A in immunity and autoimmune diseases: Compelling evidence for targeted therapy. *Expert Opin. Ther. Targets* **26**, 461–477 (2022).

16. F. Hu, X. Jiang, C. Guo, Y. Li, S. Chen, W. Zhang, Y. Du, P. Wang, X. Zheng, X. Fang, X. Li, J. Song, Y. Xie, F. Huang, J. Xue, M. Bai, Y. Jia, X. Liu, L. Ren, X. Zhang, J. Guo, H. Pan, Y. Su, H. Yi, H. Ye, D. Zuo, J. Li, H. Wu, Y. Wang, R. Li, L. Liu, X. Y. Wang, Z. Li, Scavenger receptor-A is a biomarker and effector of rheumatoid arthritis: A large-scale multicenter study. *Nat. Commun.* **11**, 1911 (2020).

17. Y. Xie, X. Jiang, P. Wang, X. Zheng, J. Song, M. Bai, Y. Tang, X. Fang, Y. Jia, Z. Li, F. Hu, SR-A neutralizing antibody: Potential drug candidate for ameliorating osteoclastogenesis in rheumatoid arthritis. *Clin. Exp. Immunol.* **207**, 297–306 (2022).

18. C. Wei, P. Wang, J. Zhang, X. Jiang, Y. Xie, Y. Li, W. Zhang, Y. Du, X. Zheng, X. Fang, S. Liu, L. Cao, R. Yao, X. Jin, D. Zhu, H. Wu, Y. Wang, Z. Li, F. Hu, Combination of scavenger receptor-A with anti-cyclic citrullinated peptide antibody for the diagnosis of rheumatoid arthritis. *Rheumatology* keae297 (2024).

19. Y. Qian, Y. Wang, X. Zhang, L. Zhou, Z. Zhang, J. Xu, Y. Ruan, S. Ren, C. Xu, J. Gu, Quantitative analysis of serum IgG galactosylation assists differential diagnosis of ovarian cancer. *J. Proteome Res.* **12**, 4046–4055 (2013).

20. P. Umaña, J. Jean-Mairet, R. Moudry, H. Amstutz, J. E. Bailey, Engineered glycoforms of an antineuroblastoma IgG1 with optimized antibody-dependent cellular cytotoxic activity. *Nat. Biotechnol.* **17**, 176–180 (1999).

21. D. Aletaha, J. S. Smolen, Diagnosis and management of rheumatoid arthritis: A review. *JAMA* **320**, 1360–1372 (2018).

22. C.-Q. Chu, Preventing rheumatoid arthritis: Lessons from that of type 1 diabetes. *Rheumatol. Autoimmun.* **3**, 67–69 (2023).

23. H. Koppejan, L. A. Trouw, J. Sokolove, L. J. Lahey, T. J. W. Huizinga, I. A. Smolik, D. B. Robinson, H. S. El-Gabalawy, R. E. M. Toes, C. A. Hitchon, Role of anti–carbamylated protein antibodies compared to anti–citrullinated protein antibodies in indigenous north americans with rheumatoid arthritis, their first-degree relatives, and healthy controls. *Arthritis Rheum.* **68**, 2090–2098 (2016).

24. M. Juarez, H. Bang, F. Hammar, U. Reimer, B. Dyke, I. Sahbudin, C. D. Buckley, B. Fisher, A. Filer, K. Raza, Identification of novel antiacetylated vimentin antibodies in patients with early inflammatory arthritis. *Ann. Rheum. Dis.* **75**, 1099–1107 (2016).

25. L. Damjanovska, M. M. Thabet, E. W. N. Levarth, G. Stoeken-Rijsbergen, E. I. van der Voort, R. E. M. Toes, T. W. J. Huizinga, A. H. M. van der Helm-van Mil, Diagnostic value of anti-MCV antibodies in differentiating early inflammatory arthritis. *Ann. Rheum. Dis.* **69**, 730–732 (2010).

26. Y. Liu, C. Liu, L. Li, F. Zhang, Y. Li, S. Zhang, High levels of antibodies to citrullinated α-enolase peptide-1 (CEP-1) identify erosions and interstitial lung disease (ILD) in a Chinese rheumatoid arthritis cohort. *Clin. Immunol.* **200**, 10–15 (2019).

27. L. Martinez-Prat, D. Lucia, C. Ibarra, M. Mahler, T. Dervieux, Antibodies targeting protein-arginine deiminase 4 (PAD4) demonstrate diagnostic value in rheumatoid arthritis. *Ann. Rheum. Dis.* **78**, 434–436 (2019).

28. T. Zhu, L. Feng, Comparison of anti-mutated citrullinated vimentin, anti-cyclic citrullinated peptides, anti-glucose-6-phosphate isomerase and anti-keratin antibodies and rheumatoid factor in the diagnosis of rheumatoid arthritis in Chinese patients. *Int. J. Rheum. Dis.* **16**, 157–161 (2013).

29. Y. Wu, Z. Dai, H. Wang, H. Wang, L. Wu, H. Ling, Y. Zhu, D. Ye, B. Wang, Serum 14-3-3η is a marker that complements current biomarkers for the diagnosis of RA: Evidence from a meta-analysis. *Immunol. Invest.* **51**, 182–198 (2022).

30. J. Polmear, K. L. Good-Jacobson, Antibody glycosylation directs innate and adaptive immune collaboration. *Curr. Opin. Immunol.* **74**, 125–132 (2022).

31. D. Sun, F. Hu, H. Gao, Z. Song, W. Xie, P. Wang, L. Shi, K. Wang, Y. Li, C. Huang, Z. Li, Distribution of abnormal IgG glycosylation patterns from rheumatoid arthritis and osteoarthritis patients by MALDI-TOF-MS(n). *Analyst* **144**, 2042–2051 (2019).

32. B. Gyebrovszki, A. Ács, D. Szabó, F. Auer, S. Novozánszki, B. Rojkovich, A. Magyar, F. Hudecz, K. Vékey, L. Drahos, G. Sármay, The role of IgG Fc region N-glycosylation in the pathomechanism of rheumatoid arthritis. *Int. J. Mol. Sci.* **23**, 5828 (2022).

33. L. Hafkenscheid, E. de Moel, I. Smolik, S. Tanner, X. Meng, B. C. Jansen, A. Bondt, M. Wuhrer, T. W. J. Huizinga, R. E. M. Toes, H. El-Gabalawy, H. U. Scherer, N-linked glycans in the variable domain of IgG anti-citrullinated protein antibodies predict the development of rheumatoid arthritis. *Arthritis Rheum.* **71**, 1626–1633 (2019).

34. T. Kissel, C. Ge, L. Hafkenscheid, J. C. Kwekkeboom, L. M. Slot, M. Cavallari, Y. He, K. A. van Schie, R. D. Vergroesen, A. S. B. Kampstra, S. Reijm, G. Stoeken-Rijsbergen, C. Koeleman, L. M. Voortman, L. H. Heitman, B. Xu, G. J. M. Pruijn, M. Wuhrer, T. Rispens, T. W. J. Huizinga, H. U. Scherer, M. Reth, R. Holmdahl, R. E. M. Toes, Surface Ig variable domain glycosylation affects autoantigen binding and acts as threshold for human autoreactive B cell activation. *Sci. Adv.* **8**, eabm1759 (2022).

35. Y. Ohmi, W. Ise, A. Harazono, D. Takakura, H. Fukuyama, Y. Baba, M. Narazaki, H. Shoda, N. Takahashi, Y. Ohkawa, S. Ji, F. Sugiyama, K. Fujio, A. Kumanogoh, K. Yamamoto, N. Kawasaki, T. Kurosaki, Y. Takahashi, K. Furukawa, Sialylation converts arthritogenic IgG into inhibitors of collagen-induced arthritis. *Nat. Commun.* **7**, 11205 (2016).

36. B. Sehnert, J. Mietz, R. Rzepka, S. Buchholz, A. Maul-Pavicic, S. Schaffer, F. Nimmerjahn, R. E. Voll, Neuraminidase inhibitor zanamivir ameliorates collagen-induced arthritis. *Int. J. Mol. Sci.* **22**, 1428 (2021).

37. M. M. Chang, L. Gaidukov, G. Jung, W. A. Tseng, J. J. Scarcelli, R. Cornell, J. K. Marshall, J. L. Lyles, P. Sakorafas, A.-H. A. Chu, K. Cote, B. Tzvetkova, S. Dolatshahi, M. Sumit, B. C. Mulukutla, D. A. Lauffenburger, B. Figueroa Jr., N. M. Summers, T. K. Lu, R. Weiss, Small-molecule control of antibody N-glycosylation in engineered mammalian cells. *Nat. Chem. Biol.* **15**, 730–736 (2019).

38. A. Damerau, M. Pfeiffenberger, M.-C. Weber, G.-R. Burmester, F. Buttgereit, T. Gaber, A. Lang, A human osteochondral tissue model mimicking cytokine-induced key features of arthritis in vitro. *Int. J. Mol. Sci.* **22**, 128 (2021).

39. U. Harre, D. Georgess, H. Bang, A. Bozec, R. Axmann, E. Ossipova, P.-J. Jakobsson, W. Baum, F. Nimmerjahn, E. Szarka, G. Sarmay, G. Krumbholz, E. Neumann, R. Toes, H.-U. Scherer, A. I. Catrina, L. Klareskog, P. Jurdic, G. Schett, Induction of osteoclastogenesis and bone loss by human autoantibodies against citrullinated vimentin. *J. Clin. Invest.* **122**, 1791–1802 (2012).

40. G. M. Thiele, M. J. Duryee, A. Dusad, C. D. Hunter, J. P. Lacy, D. R. Anderson, D. Wang, J. R. O'Dell, T. R. Mikuls, L. W. Klassen, Citrullinated mouse collagen administered to DBA/1J mice in the absence of adjuvant initiates arthritis. *Int. Immunopharmacol.* **13**, 424–431 (2012).

41. K. A. Kuhn, L. Kulik, B. Tomooka, K. J. Braschler, W. P. Arend, W. H. Robinson, V. M. Holers, Antibodies against citrullinated proteins enhance tissue injury in experimental autoimmune arthritis. *J. Clin. Invest.* **116**, 961–973 (2006).

42. F. Arnoux, C. Mariot, E. Peen, N. C. Lambert, N. Balandraud, J. Roudier, I. Auger, Peptidyl arginine deiminase immunization induces anticitrullinated protein antibodies in mice with particular MHC types. *Proc. Natl. Acad. Sci. U.S.A.* **114**, E10169–E10177 (2017).

43. F. Hu, L. Shi, X. Liu, Y. Chen, X. Zhang, Y. Jia, X. Liu, J. Guo, H. Zhu, H. Liu, L. Xu, Y. Li, P. Wang, X. Fang, J. Xue, Y. Xie, C. Wei, J. Song, X. Zheng, Y.-Y. Liu, Y. Li, L. Ren, D. Xu, L. Lu, X. Qiu, R. Mu, J. He, M. Wang, X. Zhang, W. Liu, Z. Li, Proinflammatory phenotype of B10 and B10pro cells elicited by TNF-α in rheumatoid arthritis. *Ann. Rheum. Dis.* **83**, 576–588 (2024).

44. R. G. S. Chirivi, J. W. G. van Rosmalen, M. van der Linden, M. Euler, G. Schmets, G. Bogatkevich, K. Kambas, J. Hahn, Q. Braster, O. Soehnlein, M. H. Hoffmann, H. H. G. van Es, J. M. H. Raats, Therapeutic ACPA inhibits NET formation: A potential therapy for neutrophil-mediated inflammatory diseases. *Cell. Mol. Immunol.* **18**, 1528–1544 (2021).

45. Y. He, C. Ge, À. Moreno-Giró, B. Xu, C. M. Beusch, K. Sandor, J. Su, L. Cheng, E. Lönnblom, C. Lundqvist, L. M. Slot, D. Tong, V. Urbonaviciute, B. Liang, T. Li, G. F. Lahore, M. Aoun, V. Malmström, T. Rispens, P. Ernfors, C. I. Svensson, H. U. Scherer, R. E. M. Toes, I. Gjertsson, O. Ekwall, R. A. Zubarev, R. Holmdahl, A subset of antibodies targeting citrullinated proteins confers protection from rheumatoid arthritis. *Nat. Commun.* **14**, 691 (2023).

46. M. C. Jespersen, B. Peters, M. Nielsen, P. Marcatili, BepiPred-2.0: Improving sequence-based B-cell epitope prediction using conformational epitopes. *Nucleic Acids Res.* **45**, W24–W29 (2017).

47. S. Sun, C. Huang, Y. Wang, Y. Liu, J. Zhang, J. Zhou, F. Gao, F. Yang, R. Chen, B. Mulloy, W. Chai, Y. Li, D. Bu, Toward automated identification of glycan branching patterns using multistage mass spectrometry with intelligent precursor selection. *Anal. Chem.* **90**, 14412–14422 (2018).

48. C. Huang, M. Hou, J. Yan, H. Wang, Y. Wang, C. Cao, Y. Wang, H. Gao, X. Ma, Y. Zheng, D. Bu, W. Chai, Y. Li, S. Sun, GIPS-mix for accurate identification of isomeric components in glycan mixtures using intelligent group-opting strategy. *Anal. Chem.* **95**, 811–819 (2023).

49. C. Huang, H. Wang, D. Bu, J. Zhou, J. Dong, J. Zhang, H. Gao, Y. Wang, W. Chai, S. Sun, Y. Li, Multistage mass spectrometry with intelligent precursor selection for N-glycan branching pattern analysis. *Carbohydr. Polym.* **237**, 116122 (2020).

50. P. Occhetta, S. Pigeot, M. Rasponi, A. Dasen, A. Mehrkens, T. Ullrich, I. Kramer, S. Guth-Gundel, A. Barbero, I. Martin, Developmentally inspired programming of adult human mesenchymal stromal cells toward stable chondrogenesis. *Proc. Natl. Acad. Sci. U.S.A.* **115**, 4625–4630 (2018).

51. C. Guo, F. Hu, H. Yi, Z. Feng, C. Li, L. Shi, Y. Li, H. Liu, X. Yu, H. Wang, J. Li, Z. Li, X.-Y. Wang, Myeloid-derived suppressor cells have a proinflammatory role in the pathogenesis of autoimmune arthritis. *Ann. Rheum. Dis.* **75**, 278–285 (2016).

52. D. D. Brand, K. A. Latham, E. F. Rosloniec, Collagen-induced arthritis. *Nat. Protoc.* **2**, 1269–1275 (2007).